Effect of water table variations and input of natural organic matter on the cycles of C and N, and mobility of As, Zn and Cu from a soil impacted by the burning of chemical warfare agents: A mesocosm study

Hugues Thouin, Fabienne Battaglia-Brunet, Pascale Gautret, Lydie Le Forestier, Dominique Breeze, Fabienne Séby, Marie-Paule Norini, Sébastien Dupraz

HAL Id: insu-01508666
https://insu.hal.science/insu-01508666

Submitted on 14 Apr 2017

1   **Effect of water table variations and input of natural organic matter on the**
2   **cycles of C and N, and mobility of As, Zn and Cu from a soil impacted by the**
3   **burning of chemical warfare agents: a mesocosm study.**

4   Hugues Thouin [a,b,c,d], Fabienne Battaglia-Brunet [a,b,c,d], Pascale Gautret [b,c,d], Lydie Le Forestier
5   [b,c,d], Dominique Breeze [a], Fabienne Séby [e], Marie-Paule Norini [b,c,d], Sebastien Dupraz [a].

6   [a] BRGM, 3 avenue Claude Guillemin, 45060 Orléans, France
7   [b] Université d'Orléans, ISTO, UMR 7327, 45071 Orléans, France
8   [c] CNRS, ISTO, UMR 7327, 45071 Orléans, France
9   [d] BRGM, ISTO, UMR 7327, BP 36009, 45060 Orléans, France
10 [e] UT2A, Hélioparc Pau Pyrénées, 2 avenue du président Angot, 64053 Pau, France

11 **Highlights**

12 • Monitoring of contaminants submitted to a change of environmental conditions.

13 • Saturation and desaturation cycle had the most marked impact on nitrogen cycle.

14 • The addition of organic matter increased As III mobility in saturated condition.

15 • These sites provide As and Zn stock for hundred years of environmental pollution.

16 **Graphical abstract**
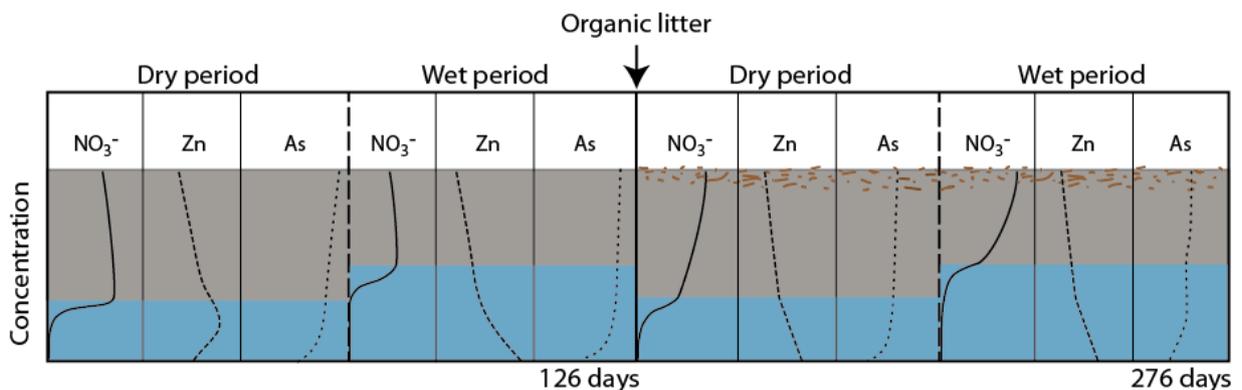
17

18

19 **Abstract**

20 A mesocosm study was conducted to assess the impact of water saturation episodes and of the

21 input of bioavailable organic matter on the biogeochemical cycles of C and N, and on the

22 behavior of metal(loid)s in a soil highly contaminated by the destruction of arsenical shells. An

23 instrumented mesocosm was filled with contaminated soil taken from the "Place-à-Gaz" site.

Four cycles of dry and wet periods of about one month were simulated for 276 days. After two dry/wet cycles, organic litter sampled on the site was added above the topsoil. The nitrogen cycle was the most impacted by the wet/dry cycles, as evidenced by a denitrification microbial process in the saturated level. The concentrations of the two most mobile pollutants, Zn and As, in the soil water and in the mesocosm leachate were, respectively, in the 0.3–1.6 mM and 20-110 µM ranges. After 8 months of experiment, about 83 g.m^{-3} of Zn and 3.5 g.m^{-3} of As were leached from the soil. These important quantities represent less than 1 % of the solid stock of this contaminant. Dry/wet cycles had no major effect on Zn mobility. However, soil saturation induced the immobilization of As by trapping As V but enhanced As III mobility. These phenomena were amplified by the presence of bioavailable organic matter. The study showed that the natural deposition of forest organic litter allowed a part of the soil's biological function to be restored but did not immobilize all the Zn and As, and even contributed to transport of As III to the surrounding environment. The main hazard of this type of site, contaminated by organo-arsenic chemical weapons, is the constitution of a stock of As that may leach into the surrounding environment for several hundred years.

1. Introduction

Soils contaminated by inorganic pollutants can lose some or all of their functions but they may also evolve under the influence of forcing factors such as climate, presence of organisms or human activity, and can spontaneously recover some functions when colonized by vegetation (Huot *et al.,* 2015). Contaminated soils may contain large amounts of metals and metalloids whose fate is directly dependent on their evolution and function.

Modern warfare is a source of environmental pollution, and has been found to have highly negative effects on the structure and functioning of ecosystems (Lawrence *et al*., 2015). Chemical weapons containing nitroaromatic, chlorine, bromine and arsenical compounds, were used on a massive scale. Aromatic arsenicals (AAs), such as ADAMSITE (10-chloro-5,10-dihydrophenarsine), CLARK I (diphenylchloroarsine), CLARK II (diphenylcyanoarsine), and PFIFFIKUS (phenyldichloroarsine) were mainly produced as vomiting or vesicant agents during World Wars I and II. After the conflicts, the remaining weapons were either burned, or abandoned in Europe, China, Japan, and other countries by sea-dumping or earth-burying (Bausinger and Preuβ, 2005). The mother molecules or their degradation products were detected in soils, plants, sediments and groundwater (Bada *et al*., 2008, Daus *et al*., 2010, Certini *et al*., 2013). The behavior of these arsenic species is controlled by environmental factors.

Dissolved organic matter was shown to mobilize arsenic from iron oxides in soils and sediments, as a result of both competition between arsenic and organic anions for sorption sites, and redox reactions (Bauer and Blodau, 2006; Dobran and Zagury, 2006).

Soil saturation can affect biogeochemical cycles, such as those of carbon and nitrogen (Rey *et al*., 2005; Rubol *et al*., 2012; Parson *et al*., 2013; Anderson *et al*., 2014) and, more generally, all reactions influenced by the oxygen availability (Silver *et al*., 1999; Dutta *et al*., 2015) and

the redox conditions of the environment. Organic matter biodegradation is affected by soil water content, excess water reducing microbial activity (Kowalenko *et al.,* 1978), 60% water holding capacity being generally considered as the optimum moisture content for microbial respiration (Howard and Howard, 1993). More generally, moisture is one of the most important factors that affect microbial community structure and processes in soils (DeAngelis *et* al., 2010 ; Rodrigo *et al*., 1997), the percentage of soil space filled with water being the best indicator of aerobic/anaerobic microbial activity (Linn and Doran, 1984). Concerning the cycle of nitrogen, experiments and models indicate an optimum of ammonification and nitrification activities with moisture close to 60%, and increase of denitrification activity at higher values of soil moisture, up to water saturation (Rodrigo *et al*., 1997). Considering other anaerobic nitrogen transformations, dissimilatory nitrate reduction to ammonium (DNRA) increases with soil saturation but was observed in soils presenting 50-60% moisture (Silver *et al*., 2001), whereas ammonium oxidation coupled to ferric iron reduction (Feammox) is considered to occur only in strictly anaerobic conditions (Yang *et al*., 2012). However, anoxic microsites can allow anaerobic microbial reaction in soils that are not water saturated (Silver *et al*., 2001). Saturation of the soil by water can influence the behavior of metals and metalloids in polluted soils as a result of the change in redox conditions. Many authors have observed that As solubility increases in saturated soils because of the joint dissolution of iron oxides and reduction of AsV (Kumpiene *et al*., 2009; Weber *et al*., 2010; Couture *et al*., 2015). Anaerobic microbial reduction of Fe(III) and Mn(IV) may induce release of metals such as Cu or Zn, and this process may be enhanced by soil polymers like humic materials, related compounds, and organic acids produced by organic matter degradation (Gadd 2004).

Biogeocycles are influenced not only by the saturation level but also by its temporal dynamics. Thus, carbon mineralization rate was shown to be stimulated in the zones of cyclic variation of groundwater table (Banks *et al*., 1999, Blodau and Moore, 2003). Enhanced substrate release

1 due to redox-induced chemical breakdown and enhanced recycling of biomass after the redox

2 disturbance explain the stimulation of biogeochemical processes in these zones (Aller, 1994).

3 Studies describing As behavior during redox oscillation (Parsons *et al*., 2013, Couture *et al*.,

4 2015) have shown that the successive cycles of oxidizing and reducing conditions affect As

5 mobility in relation with As speciation and sorption onto hydrous ferric oxide (HFO). The

6 mobility of metals such as Cu and Zn is also related to iron dissolution related to oscillation of

7 redox conditions (Schulz-Zunkel *et al*., 2015).

8 Here, the influence of organic matter supply and water saturation status on the dynamics of As

9 and metals was studied in a soil highly polluted by the destruction of chemical weapons. During

10 the 1920–1928 period, 200,000 shells were broken down and open-burned near Verdun

11 (France), on a site named "Place-à-Gaz". The burning of Blue Cross shells – loaded with high

12 explosives coating a glass bottle containing solid diphenylchloroarsine (CLARK 1) and

13 diphenylcyanoarsine (CLARK 2) – resulted in locally intense soil contamination by arsenic and

14 heavy metals and a lack of vegetation (Bausinger *et al*., 2007; Thouin *et al*., 2016).

15 The pollution of this site has already been characterized and detailed in two studies (Bausinger

16 *et al*., 2007; Thouin *et al*., 2016), that revealed As concentrations up to 73 $g.kg^{-1}$, and

17 concentrations of Zn, Cu and Pb reaching 90 $g.kg^{-1}$, 9 $g.kg^{-1}$ and 6 $g.kg^{-1}$, respectively. Their

18 results demonstrated that the main As-carriers were amorphous materials composed of a blend

19 of metals and arsenate minerals of Zn, Cu and Fe together with the crystalline phases adamite,

20 olivenite, and two pharmacosiderites. On site, the most mobile contaminants were found to be

21 Zn – whose behavior was mainly determined by pH – and As, whose behavior was correlated

22 with the availability of iron sinks. The site is located in an oak forest and is therefore subject to

23 natural deposition of litter that provides bioavailable organic matter (OM). In addition, the

24 clayey formation beneath the contaminated soil severely limits the infiltration of rainwater and

25 favors runoff of soluble inorganic pollutants from the site. Saturation of the lower part of the

1   contaminated layer was also observed during periods of high precipitation. The stability of the

2   pollutants can therefore be altered by the evolution of environmental conditions.

3   The contaminated soil is rich in organic carbon (about 250 $g.kg^{-1}$), consisting mainly of charcoal

4   resulting from the use of firewood during destruction of the shells. However, the presence of

5   biodegradable OM at the edge of the site was also demonstrated by Thouin *et al.* (2016). The

6   two types of OM (charcoal and fresh OM) may influence the mobility of metals and metalloids,

7   either because of the high adsorption capacity of the charcoal (Hua *et al.*, 2009) or by chelation

8   or methylation processes occurring in the presence of fresh organic compounds (Park *et al.*,

9   2011; Huang *et al.*, 2012). Bioavailable OM can also promote bacterial activity and change

10   environmental conditions locally through microbial consumption of electron acceptors, thus

11   inducing redox gradients.

12   This study aimed to evaluate the effect of (i) water saturation episodes and (ii) input of

13   bioavailable OM on the behavior of pollutants that have been submitted to these environmental

14   changes for 80 years. To this end, an 8-month experiment was conducted with a 1 m^3

15   mesocosm. The originality of this work, compared with previous studies, lies in the combination

16   of its size and duration, combined with the specificity of the polluted material. A mesocosm is

17   an intermediate scale between full field scale and the laboratory microcosm. It is suitable for

18   simulating environmental events in controlled conditions and for monitoring of contaminants

19   in soil pore water. The composition of soil waters at different depths and in leachates provides

20   information on the processes that can influence the biogeocycles of carbon and nitrogen and

21   the fate of contaminants and the potential for transfer towards surrounding compartments.

22   **2. Materials and methods**

23   **2.1. Study site and soil sampling**

The study site, known as "Place-à-Gaz", is located in the Spincourt forest, 20 km northeast of Verdun, France (Bausinger *et al*., 2007; Thouin *et al*., 2016). On the site, there is a black layer of soil containing slag, coal ashes and ammunition residues resulting from the thermal destruction of arsenical shells (Bausinger *et al*., 2007; Thouin *et al*., 2016). The substrate beneath this contaminated layer is a clayey Woëvre formation of Callovian. These clays limit the infiltration of rainwater and induce the runoff together with the saturation of the lower parts of black layer.

An instrumented mesocosm was filled with about 1 m^3 of material taken from the black layer (between 0 and 30 cm) with an excavator in October 2015. The material was excavated from the most contaminated part of the site. The concentrations of the main pollutants, analyzed by NITON© X-ray fluorescence field apparatus, were 132.44 ± 3.66 g.kg^{-1}, 87.31 ± 5.08 g.kg^{-1}, 18.36 ± 0.63 g.kg^{-1}, 4.78 ± 0.19 g.kg^{-1} for As, Zn, Cu and Pb respectively. Oak organic litter was taken from the edge of the forest, close to the study site. The surface litter corresponding to the previous year's deposit was not sampled, only the thinner older organic litter was taken. It contained 305 g.kg^{-1} of total organic carbon and a C/N ratio of 21.4.

2.2. Instrumented mesocosm

The instrumented mesocosm (Fig. 1) consisted of a closed stainless steel column (1 m in diameter and 1.2 m high) filled with 610 kg of homogenized contaminated soil, placed in a temperature-regulated room at 23 ±1 °C . A layer of inert gravel (centimetric quartz and flint particles) and a geotextile membrane were disposed at the bottom of the mesocosm to facilitate outflow drainage without loss of soil particles. During filling, the column was equipped at four
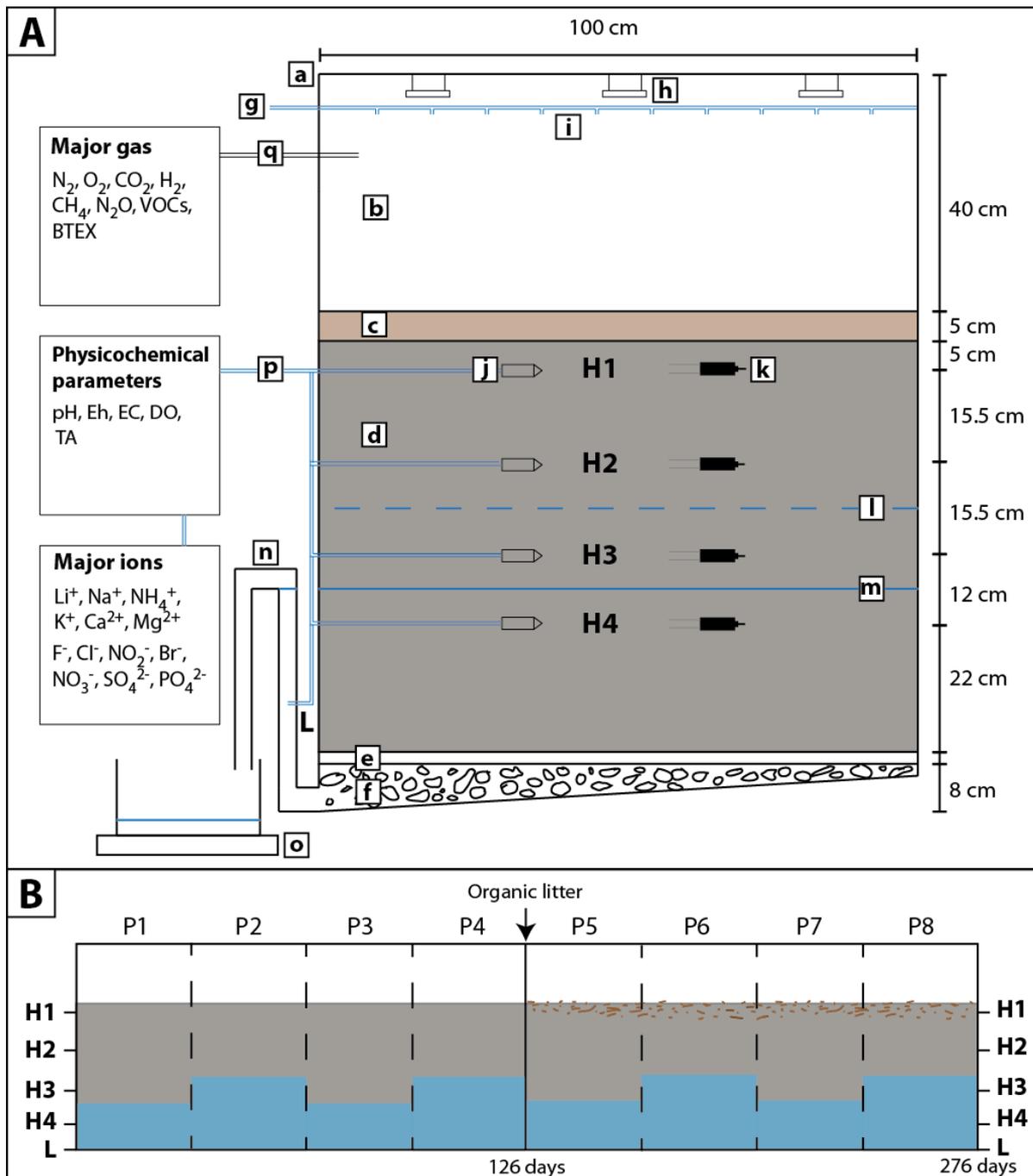
Figure 1: A. Schematic of the mesocosm experiment. a: stainless steel column, b: controlled atmosphere, c: organic litter, d: contaminated soil, e: geotextile membrane, f: inert gravel, g: feedwater, h: LED lighting, i: watering system, j: porewater samplers, k: soil moisture and temperature probes, l: water table in wet condition, m: water table in dry condition, n: water level control, o: balance, p: Fluorinated ethylene propylene water tubing, q: gas tubing. **B.** Experiment design. P1, P3, P5, P7 were dry periods, P2, P4, P6, P8 wet. From the beginning of P5 forest litter was added at the top of the contaminated soil. H4 was permanently saturated; (blue) H2 and H1 were never saturated. The H3 level was not saturated in the dry period and saturated in the wet period. The leachate (L) was sampled at the outlet of the mesocosm.

1   depths (H1: 5 cm, H2: 20.5 cm, H3: 36 cm and H4: 48 cm, measured from the top) with time

2   domain reflectometry (TDR) probes (TRIME-PICO32, IMKO), to measure soil moisture and

temperature, and with inert Polytetrafluoroethylene/Quartz porous probes (pore size 2 µm, three probes for each sampling depth) to sample soil water. These probes were inserted into the soil at 30 cm from the column wall. Five Horticultural light-emitting diode (LED) at the top of the column simulated 12-hour day/night cycles. Rainfall was simulated by a sprinkler system connected to a water reservoir and fed by two pumps. The leachate was collected in a steel tank and quantified using a weighing balance. Outflow weight and soil moisture and temperature at the four sampling levels (H1, H2, H3 and H4) were monitored continuously, with a frequency of one hour.

2.3. Experiment design

The study of vertical flows, in this instrumented mesocosm, will allow understanding the phenomena related to the water flows, constrained on the site by the clayey substrate. We consider that the flows studied in the unsaturated levels of the mesocosm are representative of the vertical flows taking place in the unsaturated zone of the polluted soil on site, and that flows in the saturated part of the mesocosm corresponds to runoff taking place at the base of the polluted layer on site. Water soil saturation effects were studied by simulation over around 8 months of cycles of dry/wet periods (P) of about one month each, referred to below as P1 to P8 (Fig.1B). The dry period was characterized by a saturation of the bottom of the mesocosm limited to the H4 level, and by the addition of around 12 L of Mont Roucous water once a week. This mineral water was used because of its chemical composition close to that of rainwater (pH = 6.38, electrical conductivity = 160 µS.cm^{-1}, Cl$^-$ = 56 µM, NO$_3^-$ = 24 µM, SO$_4^{2-}$ = 16 µM, Na$^+$ = 109 µM, K$^+$ = 7.7 µM, Ca^{2+} = 25 µM, Mg^{2+} = 21 µM). The wet period was characterized by elevation of the water table in order to saturate both H3 and H4 levels, and by the addition of 6 L of water every two days. After two dry-period/wet-period cycles (day 126), 24 kg of fresh organic forest litter taken from the "Place-à-Gaz" site was added above the topsoil in order to study the impact of a supply of fresh OM. The mesocosm atmosphere was controlled and

9

1   renewed by wet compressed air (N_2 = 82.45 ± 0.15 %, O_2 = 22.68 ± 6.7 10^{-2} % and CO_2 =

2   0.053 ± 6.7 10^{-4}%) at a flow rate of 60 L.h^{-1} for the duration of the experiment.

2.4. Sampling and analyses of soil water and leachate

4   Sampling of soil waters from levels H2, H3, H4 (not from H1 because this level did not contain

5   enough water) and of the mesocosm leachate L was performed twice a week (before sprinkle)

6   via fluorinated ethylene propylene (FEP) tubing connected to a peristaltic pump. Major ions

7   and physicochemical parameters of water samples were measured directly. Electrical

8   conductivity (EC), redox potential (Eh), pH, dissolved oxygen (DO), and temperature of

9   interstitial water were measured with a benchtop meter (multiparameter analyzer C3040,

10   Consort) connected to an ORP sensor (platinum electrode, with a Ag/AgCl reference electrode,

11   3M KCl, Eh value refers to the normal hydrogen electrode (NHE)), oxygen probes

12   (Fisherbrand), pH electrode (Fisherbrand) and conductivity probe (Sentek). Total alkalinity

13   (TA) of the leachate was measured by titration, with the 848 Titrino plus (Metrohm).

14   Major ions (Li^+, Na^+, NH_4^+, K^+, Ca^{2+}, Mg^{2+}, F^-, Cl^-, NO_2^-, Br^-, NO_3^-, SO_4^{2-}, PO_4^{3-}) were

15   analyzed and quantified by ion chromatography (IC) using a 940 Professional IC Vario

16   instrument (Metrohm, Herisau, Switzerland) equipped with conductivity detectors. Anions

17   were separated with a Metrosep A Supp 16 ionic resin column (150 mm × 4 mm i.d.) and

18   cations with a Metrosep C6 (150 mm × 4 mm i.d.). The quantification limits and precision of

19   all analytical methods are presented in supplementary material SM.6.

20   In addition, trace element concentrations (As, metals) and dissolved organic carbon (DOC)

21   were determined once a week. The soil water samples were filtered at 0.45 µm and As

22   speciation was performed immediately with an ion exchange method (Kim, 2001). Separation

23   was performed on anionic resin (AG 1-X8©, Biorad, Hercules, CA, USA). In these conditions

24   (pH < 9.3), this method separates non charged species, such as As III, from anionic species

1   including As V. Data obtained with this method were presented as As III-like and As V-like

2   species. A water sample was acidified for determination of total As, Fe, Cu, Zn and Pb. Arsenic

3   and metals were quantified with an Atomic Absorption Spectrometry oven (AAS; Varian, Palo

4   Alto, CA, USA). DOC concentration was measured using a TOC 5050/SSM 5000-A

5   (Shimadzu) elemental analyzer.

6   As speciation in soil waters was determined once a month by HPLC-ICP MS. Chromatographic

7   separation was carried out with a Model 1100 HPLC pump (Agilent, Wilmington, DE, USA)

8   as the delivery system. The exit of the column was connected directly to the Meinhard nebulizer

9   (Glass Expansion, Romainmotier, Switzerland) of the ICP MS (Agilent 7500cx, Tokyo, Japan)

10 via PEEK tubing. Injections were performed using a Rheodyne valve with a 100 µL loop.

11 Arsenic species separation was performed using an anion exchange column (Hamilton PRP-

12 X100 – 250 mm x 4.1 mm). The mobile phase used was a carbonate based gradient at pH 8.9

13 (20 mM from 0 to 10 min and 50 mM from 10 to 25 min). This allowed determination of

14 arsenobetaine, As III, As V and methylated As species (DMAA and MMAA). Phenylated As

15 compounds (courtesy of Lionel Lumet, Laboratoire de l'Environnement et de la Vendée,

16 France) such as diphenylarsinic acid (DPAA), triphenylarsine oxide (TPAO) and

17 triphenylarsine (TPA) were also injected but were not eluted from the column in these

18 conditions. Concentration values and uncertainties found were calculated from a duplicate

19 determination.

20 A previous study has described the presence on the site of nitroaromatic and organoarsenical

21 compounds (Bausinger *et al*., 2007). Twenty five nitroaromatic and six aromatic arsenical

22 compounds were searched in the contaminated soil and the mesocosm leachate at the end of the

23 experiment (P8) by a specialized laboratory (Envilytix, Wiesbaden, Germany) Nitroaromatic

24 compounds were analyzed according to ISO 11916-1 (2013) and KORA-TV 5 method (Joos *et*

25 *al*., 2008). Diphenylarsinic acid was analyzed by HPLC-DAD and cacodylic acid, clark I, clark

II, triphenylarsine, 9-phenylarsafluorene were analyzed by GC-MS applying the method detailed in Bausinger and Preuβ (2005) and Bausinger *et al*. (2007).

2.5. Gas analyses of atmosphere and respiratory test

CO_2, O_2, H_2, N_2, N_2O, CO and CH_4 as well as light hydrocarbons in the atmosphere of the mesocosm were analyzed online, every week, using a gas chromatograph (Compact GC Interscience, CPG) equipped with three columns and detectors in parallel, with He as carrier gas. H_2, O_2, N_2, and CO were separated in an Rt-Msieve 5A column (5A, 15 m $\times$ 0.32 mm) and CO_2, CH_4 and N_2O were separated in a HayeSep D column (30 m $\times$ 0.32 mm). Gaseous species were analyzed by thermal conductivity detector (TCD). In the third column (Stabilwax, 12 m $\times$ 0.32 mm), volatile organic carbon (VOC) and BTEX were separated and analyzed by flame ionization detection (FID). The gas chromatograph was linked directly to the column atmosphere via 0.8–1.6 mm (1/16) PEEK capillary tubing.

The mineralization of CO_2 by the mesocosm was evaluated 6 times, at the end of each period with the exception of P1 and P2. The increase of CO_2 in the column atmosphere was measured in dark conditions and without input of atmospheric air. CO_2 concentrations were analyzed about every 7 minutes over 3 hours. Carbon mineralization rates were calculated from the linear increase of CO_2 concentration in the column over time.

Arsine gases, including arsine, monomethylarsine (MeAsH$_2$), dimethylarsine (Me$_2$AsH) and trimethyl arsine (TMAs), were quantified at the end of each period P using the method from Mestrot et al. (2009). Arsines were trapped on silver nitrate impregnated silica gel containing tubes connected to the outlet of the mesocosm for 3 days. Traps were eluted with 5 mL of boiling water. Concentrated hydrogen peroxide (100 µL) was added to the eluate in order to respectively oxidize TMAs to trimethylarsine oxide (TMAO), Me$_2$AsH to dimethylarsinic acid (DMAA), MeAsH$_2$ to monomethylarsonic acid (MMAA) and arsenite to arsenate, for further

determination. Solutions obtained from the gaseous traps were determined by HPLC-ICP MS in the elution conditions given in Mestrot *et al.* (2009) using a phosphate buffer (10 mM pH 6.2) as mobile phase. These conditions allow the determination of TMAO, DMAA, MMAA and As(V) in solutions originally corresponding to the following gaseous arsines (TMAs, Me_2AsH, $MeAsH_2$ and AsH_3, respectively) after their oxidation

2.6. Leaching tests

In parallel to the mesocosm experiment, leaching tests were performed to estimate the mobility of major compounds, metals and arsenic from the different solid materials used in this study. Tests were performed with solid/liquid ratios from 1 to 10 (wet solid equivalent to 10 g of dry weight, 100 mL of Mont Roucous water in tubes) for both materials: polluted soil (similar to soil mesocosm, "Soil") and forest litter ("OM"). Tubes were rotated on a roller mixer for 24h at 20°C. All conditions were performed in triplicates. Chemical parameters, ions, metals and arsenic concentrations were measured by methods previously described.

2.7. Statistical analyses

All statistical tests were conducted in R 3.2.4 (www.r-project.org). To summarize temporal trends of element concentration, values were plotted with a smooth curve based on the loess function (ggplot 2 package). The Loess function is a smooth local regression for "geom_smooth" in the ggplot2 package for a small sample size; it is controlled by the "span" setting (Wickham, 2009) ranging from 0 (exceedingly "wiggly" smooth curve) to 1 (less "wiggly" smooth curve). In this study, span was set between 0.3 and 0.4, depending on the variation of the temporal data.

Overall trends, without the effect of dry/wet cycles, were also statistically tested using the Seasonal Kendall (SK) test (Hirsch *et al*., 1982; Hirsch and Slack, 1984), which is a modified version of the non-parametric Mann Kendall test (Mann, 1945; Kendall, 1948) for monotonic trend. The SK test, which is robust to outliers and missing values, can be used considering inner

dependence of data. The seasonal effect (here the shift between dry and wet periods) is reduced

by making comparisons between data from a similar season (period). Kendall's tau (τ) measures

the degree of correspondence between two variables. If $\tau = 0$ no correlation exists between the

pairs, if τ is positive there is an upward trend and a negative τ is associated with a downward

trend. The statistical significance of the trend is indicated by the corresponding p-value ($p \leq$

0.05 is considered significant). The statistical parameters τ and p-value were shown on the

curves exclusively for significant trends. All results of SK test are given in SM.4.

Results from leaching tests were tested for homogeneity of variance and normality. One-way

analysis of variance and Tukey tests were carried out to test for any differences between each

treatment. For each treatment the number of observations was equal to 3, and a difference of

5% between means ($p \leq 0.05$) is considered significant.

3. Results

3.1. Composition of soil water and leachate

3.1.1. Physicochemical parameters

The physicochemical parameters of water (pH, EC, Eh and DO) for the 3 levels of soil waters

and leachate are shown in Figure 2. Soil waters and leachate were characterized by pH values

between 5.5 and 6.0 at all of the different depths of soil water and throughout the experiment.

Leachates were slightly more acid than the soil waters. Electrical conductivity ranged from 500

to 2,500 μS.cm^{-1}. EC increased with depth and was highest in the leachate. In the samples from

each level, the maximum EC was measured in the first or second period and decreased until the

end of the experiment.
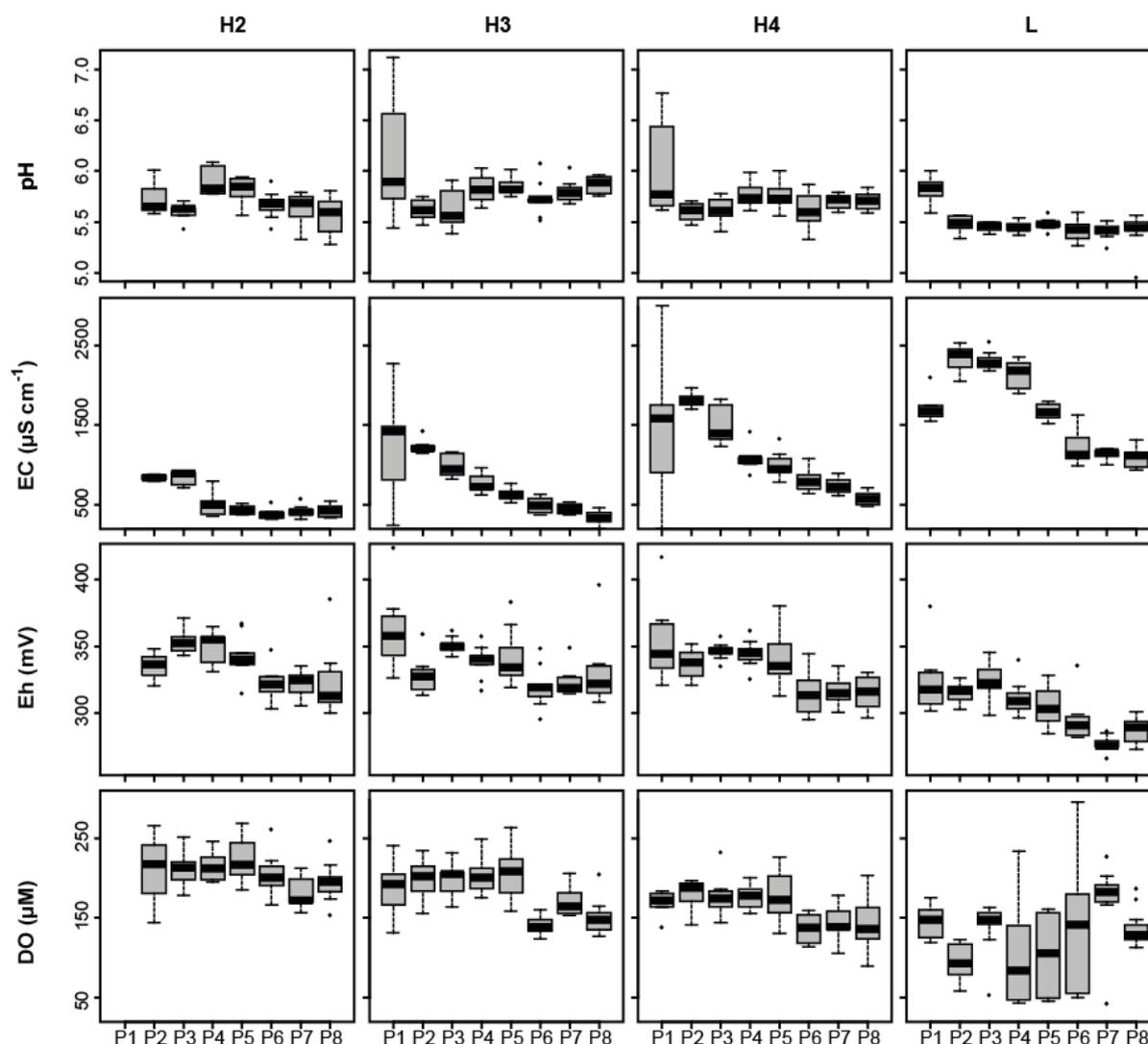
Figure 2: Evolution of physicochemical parameters in each sampling level. Boxplots represent the median, 25th percentile and the 75th percentile, error bars indicate 10th and 90th percentile. Data not included between the whiskers were plotted as an outlier. Each boxplot includes values of one period P (n = 5–10).

1

2　The redox potential (Eh) varied between 270 and 380 mV, indicating moderately oxidized soil

3　waters and leachates. Eh was stable during the first 4 periods and then decreased, particularly

4　in H4 and L. DO varied between 250 and 160 µM in H2 to 180 and 140 µM in H4. In H3 and

5　H4, DO was lower in P6–P8 than in P1–P5 (about 180 to 140 µM). DO in the leachate fluctuated

6　widely between 200 and 50 µM throughout the experiment.

7　　　**3.1.2. Major ion concentrations**

15

1   Major ions, with an average content greater than 0.05 mM, were Cl^-, NO_3^-, SO_4^{2-}, K^+, Na^+, Ca^{2+}

2   and Mg^{2+}. In order, their concentrations in soil waters were, respectively: $Cl^- > NO_3^- > SO_4^{2-}$

3   and $Ca^{2+} > Na^+ > Mg^{2+} > K^+$ (SM.5). However, NO_3^- concentrations were lower (< 0.01 mM)

4   at the bottom of the mesocosm and in the leachate. Concentrations of most of the ions analyzed

5   (Cl^-, SO_4^{2-}, K^+, Na^+, Ca^{2+}, Mg^{2+}) increased with depth and increased in the leachate in

6   accordance with EC.
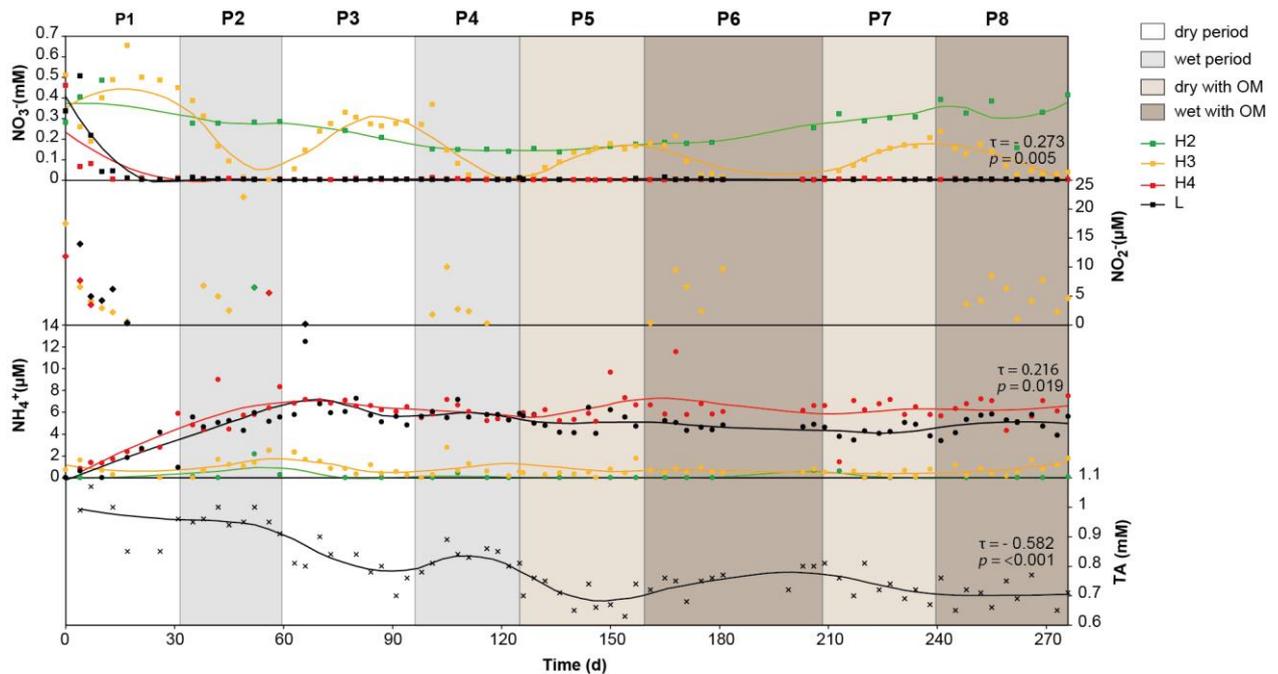
Figure 3: Measured evolution of NO_3^- (square), NO_2^- (diamond), NH_4^+ (circle) and TA (cross) concentrations. Curves correspond to smooth local regression (span = 0.3). Kendall's tau (τ) and *p*-value were given for significant trends with SK test (*p < 0.05)*.

8   The evolution of NO_3^-, NO_2^- and NH_4^+ with depth (Fig. 3) was different. In the unsaturated

9   level H2, NO_3^- concentration varied between 0.15 and 0.4 mM and for the saturated level H4

10   and the leachate L, concentration decreased quickly under 0.01 mM during the first period P1.

11   At level H3, NO_3^- concentrations increased to reach a plateau in the dry periods then decreased

12   until they disappeared in the wet periods. The maximum concentrations decreased from 0.5 mM

13   during P1 to 0.2 mM at the end of P7. This significant trend for NO_3^- concentrations was found

14   only in level H3 level ($\tau = -0.273$, $p = 0.005$). Small amounts of NO_2^- were present in the water

15   in H4 and L at the beginning of the experiment, and in H3 during each wet period. However,

16

1 except for P1, no NO_2^- was detected during dry periods. NH_4^+ concentrations showed no

2 significant trend, but two different behaviors. In H2 and H3, NH_4^+ concentrations were low (<

3 2 µM) and constant, but in H4 and L concentrations increased until 6 µM during the two first

4 periods and then remained constant.

5 Total alkalinity (TA) in the leachate decreased from 1 to 0.65 mM (Fig. 3). This decrease was

6 statistically significant based on the SK test (τ = - 0.582, $p < 0.001$). TA was subjected to

7 monthly variability and therefore increased to a local maximum during wet periods (P2, P4 and

8 P6) and decreased in dry periods (P1, P3 and P5). These variations were narrower in the last

9 two periods, P7 and P8.
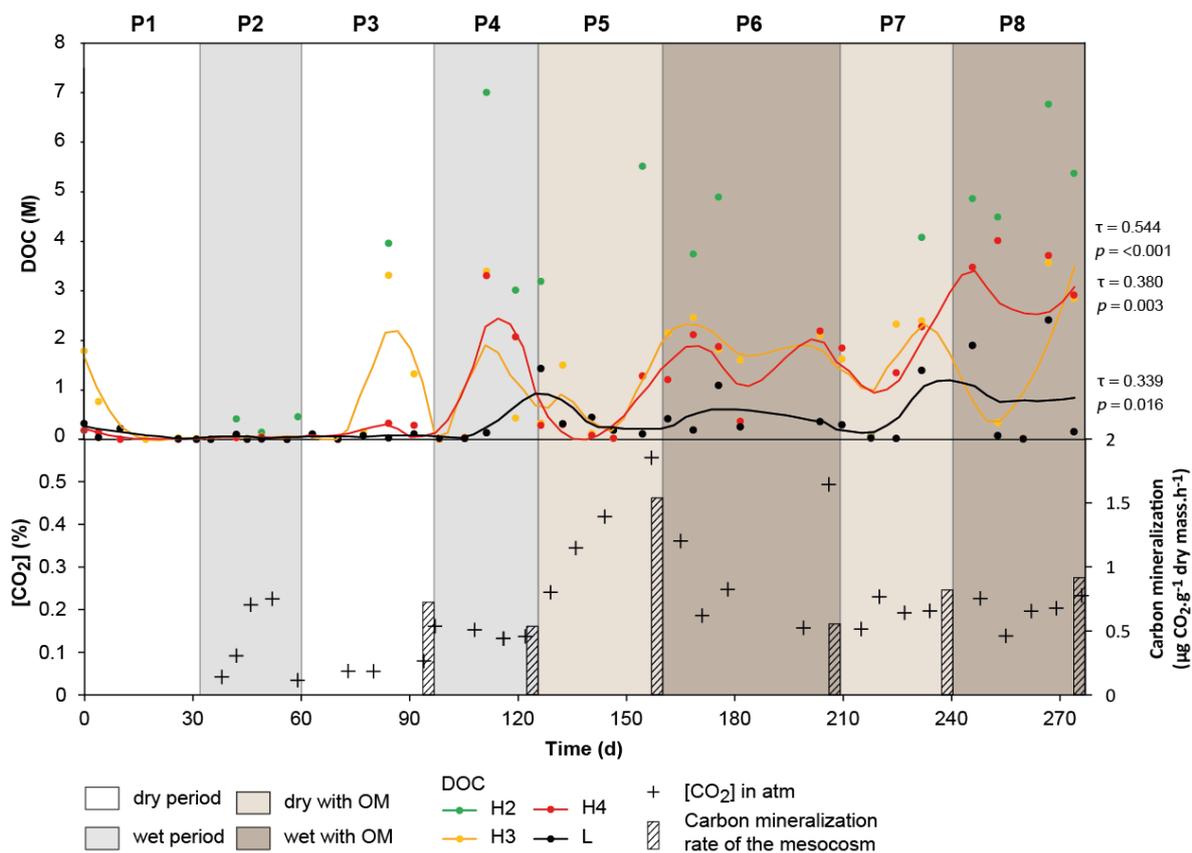
Figure 4: Evolution of DOC (circle), gaseous CO_2 in mesocosm atmosphere (cross) and carbon mineralization rate of the mesocosm (bar), measured at the end of periods P3–P8. Curves correspond to smooth local regression (span = 0.4). For H2 level sampling no local regression was calculated because of the low frequency of measurement. Kendall's tau (τ) and p-value were given for significant trends with SK test ($p < 0.05$).

10

17

Dissolved organic carbon (DOC) concentrations were very high in the soil water at level H2 (> 2 M) and decreased with depth (Fig. 4). DOC was less concentrated before the addition of forest litter, but a few samples in H2, H3 and H4 revealed high concentration peaks. After the addition of organic litter to the top of the mesocosm, DOC concentrations increased in all the samples until the end of period P8. Despite the measurement of sporadic extreme values, monthly cyclic variations are visible at each sampling level. Focusing on seasonal variability induced by dry/wet periods revealed significant positive trends in H3 ($\tau = 0.544$, $p < 0.001$), H4 ($\tau = 0.380$, $p = 0.003$) and L ($\tau = 0.339$, $p = 0.016$) (not calculated in H2 because of the low frequency of measurement).

3.1.3. Evolution of metals and arsenic concentrations

Zn was the metal with the highest concentration in soil water and leachate. Zn concentrations evolved in a similar manner at each sampling level, with an increase at the beginning of the experiment followed by a slight decrease (Fig. 5). However, a lag time was observed with depth, with maximum concentration in P1 for H2 and H3, in P2 for H3, and in P4 in the leachate. Zn also became more concentrated with depth. It seems that dry/wet cycles have no major effect on the Zn concentrations in soil water but, following the addition of fresh OM, the Zn concentration in the output water decreased sharply from 1.40 to 1.21 mM.

Cu and Fe concentrations in solution were low, with maximum amounts of about 5 µM and 40 µM , respectively (Fig. 5). Negative trends were observed in H2, H3 and L, with higher values before the addition of organic matter. In H4, Cu was mostly below the quantification limits (LQ = 1.57 µM) from P1 to P4 but, after the addition of litter, Cu concentrations in H4 were higher than at other depths. Moreover, Cu concentrations at each sampling level stabilized to a constant value after the addition of organic litter. Fe concentration increased significantly in H3, H4 and L ($\tau = 0.298$, $p = 0.035$; $\tau = 0.343$, $p = 0.011$; $\tau = 0.519$, $p < 0.001$), while negative trends were

observed in H2 ($\tau = -0.302$, $p = 0.047$). Pb concentrations were below the quantification limits

(LQ = 0.5 µM) in the soil waters.
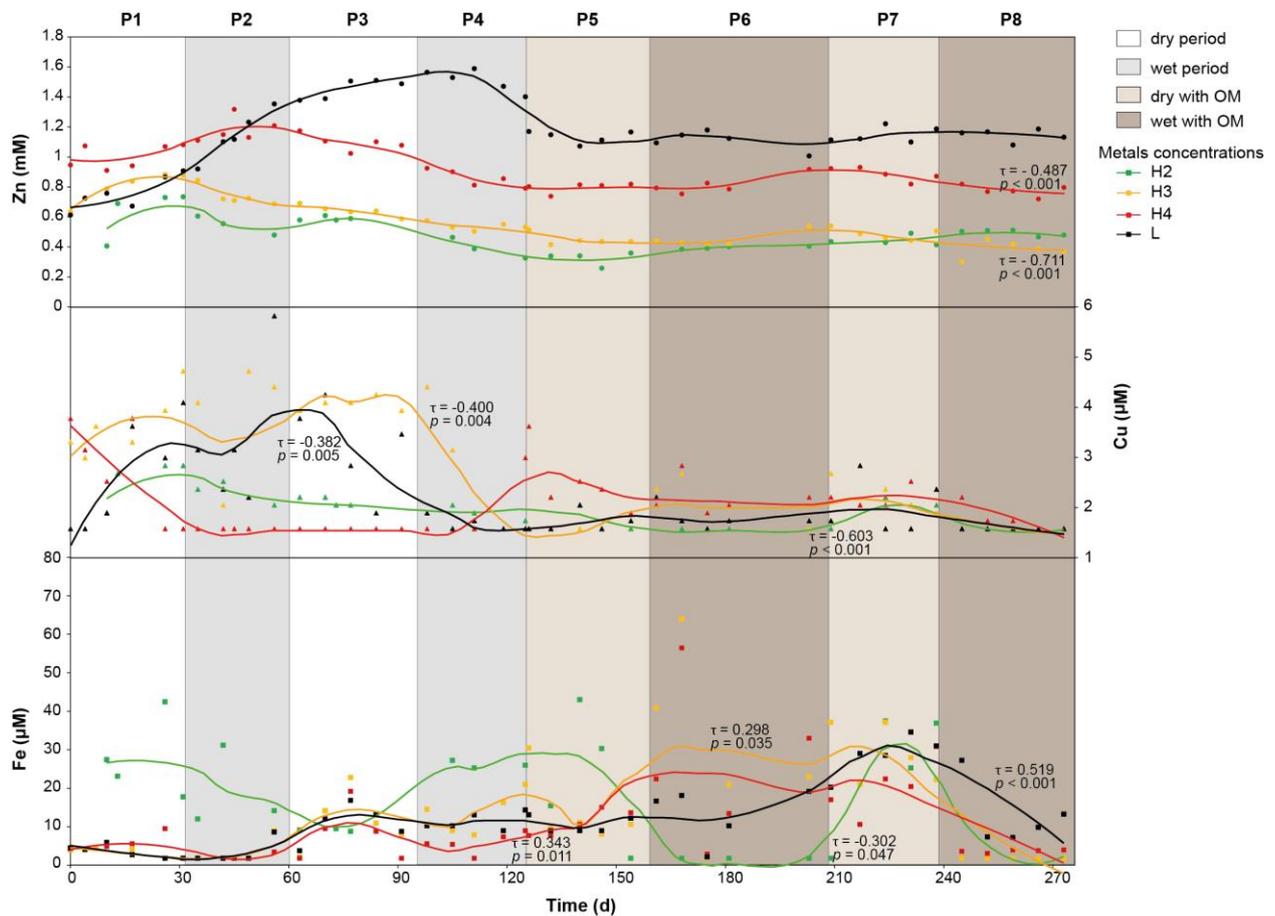
Figure 5: Evolution of concentrations of Zn (circle), Cu (triangle) and Fe (square). For Cu and Fe concentration, measurements were plotted at respectively 1.57 and 1.79 µM when value was below the quantification limit (LQ$_{Cu}$ = 1.57 µM and LQ$_{Fe}$ = 1.79 µM)). Curves correspond to smooth local regression (span = 0.3). Kendall's tau (τ) and *p*-value were given for significant trends with SK test (*p < 0.05*).

Together with Zn, As was a mobile inorganic contaminant throughout the experiment, although

the evolution of As concentration was very different: As concentrations were generally higher

in the H2 level and decreased with depth (Fig. 6). No clear impact of dry/wet period was

observed, even if monthly cycles are enhanced by the smooth curve of the data. Furthermore,

the evolution of As $_{total}$ showed significant negative trends for H2 ($\tau = -0.385$, $p = 0.033$), H4

($\tau = -0.327$, $p = 0.012$) and L ($\tau = -0.380$, $p = 0.006$), and it seems that, for soil waters, this

trend was accentuated after the addition of OM and was visible after 140 days. The same

1 evolution was observed with As V-like, which was the dominant As species in solution. At H4,

2 however, As V-like decreased more significantly (τ = -0.450; p = 0.001) than As total. As III-

3 like increased significantly (independently of the cyclical variability) in level H4 (τ = 0.398, p

4 = 0.003), especially after the addition of organic matter. In H2 and H3, As III-like concentration

5 ranged from 5 to 10 µM, with low amplitude of cyclic variation, while the concentration in L

6 ranged from 10 to 25 µM [1], with a high amplitude of monthly variation.
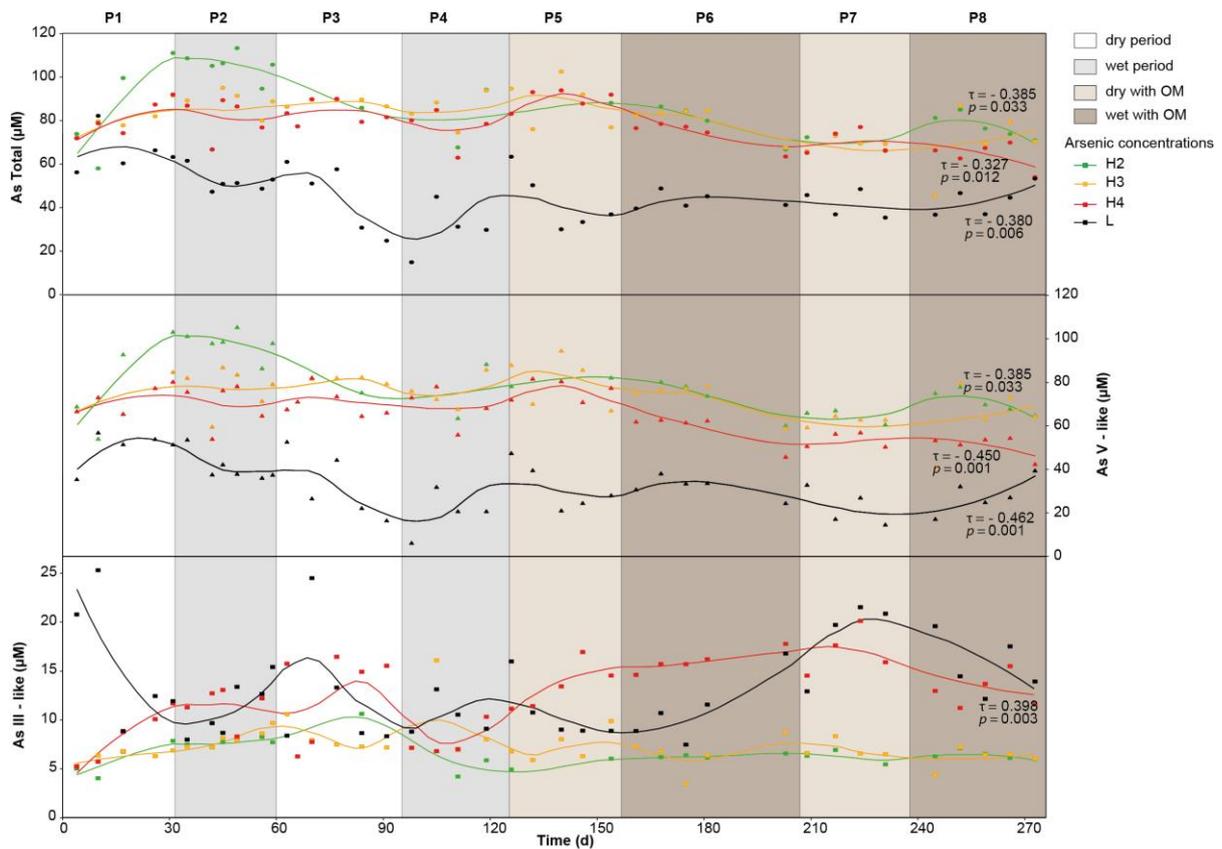
Figure 6: Evolution of concentrations of total As (circle), As V-like (triangle) and As III-like (square) obtained by separation with resin and analyses by AAS. Curves correspond to smooth local regression (span = 0.3). Kendall's tau (τ) and *p*-value were given for significant trends with SK test (*p < 0.05*).

7

8 Results of arsenic speciation obtained with HPLC-ICP MS in water from H2, H3 and H4 (Fig.

9 7) show that As V concentration presents a distribution similar to that of As V measured as total

10 As after separation on anionic resin. Conversely, As III concentrations measured with HPLC-

11 ICP MS were lower. Four other As species were detected in soil water. Diphenylarsinic acid

20

1   (DPAA) was identified and quantified in the mesocosm leachate at the end of the experiment

2   (P8), its concentration reaching $30.6\,\mu g.L^{-1}$ (SM.2). Three unidentified species were also

3   detected. Concentrations of the first unidentified compound ranged from 2 to 2.5 µM and were

4   very homogeneous over all of the sampling levels and each of the periods. Unidentified 1 was

5   the third main arsenic species after As V and As III in terms of concentration. The second

6   unidentified compound was only detected in H4 and L, with concentrations increasing from

7   about 1 to 2.5 µM, and in H3 during the wet periods (P2, P4, P6 and P8). A third unidentified

8   compound was detected in the leachate L and at all depths, however, it could not be quantified

9   because of its lesser concentrations.
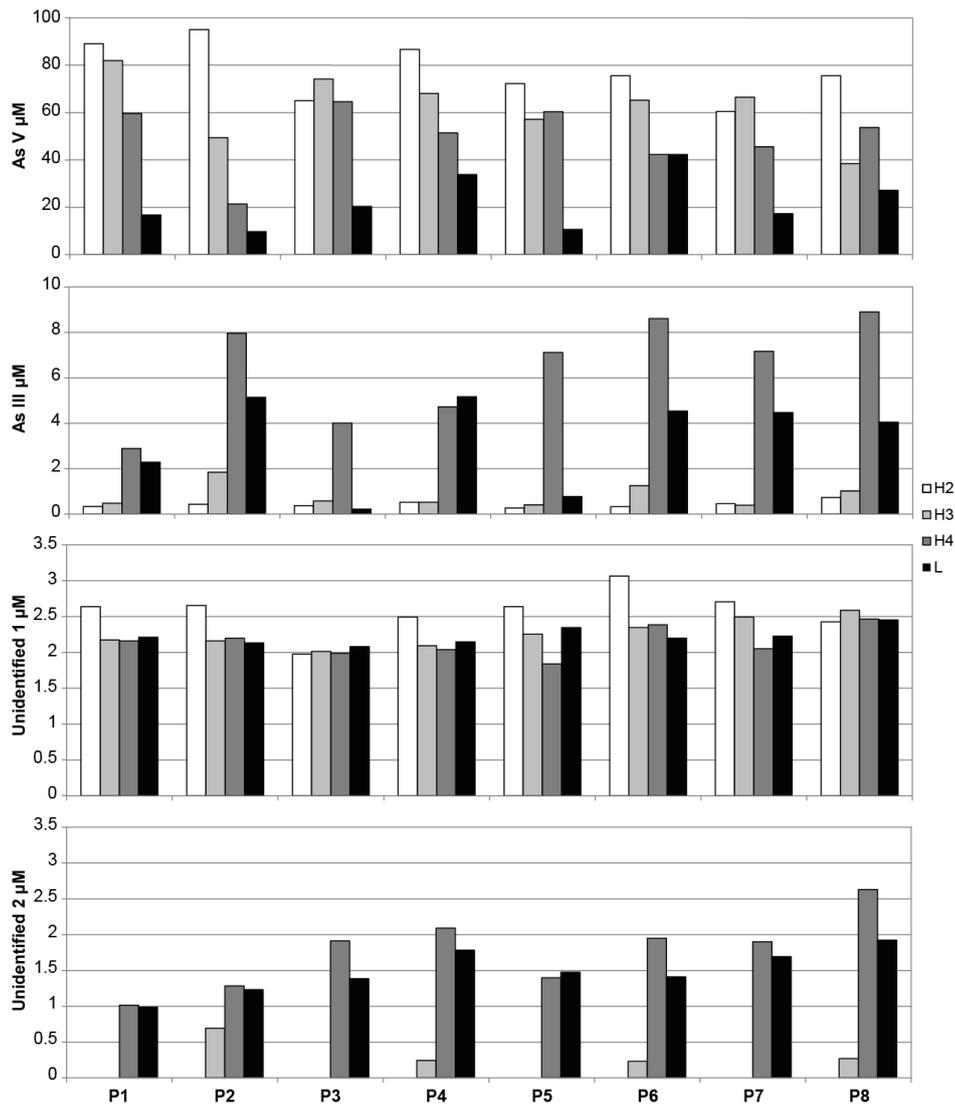
Figure 7: Arsenic speciation in soil water samples at the end of each period measured with HPLC-ICP MS. Unidentified 1 and unidentified 2 were unidentified As species. Their concentrations were evaluated from calibration of other species and are only indicative. (LQ = 1.3 10^{-3} µM for As III and LQ = 6.7 10^{-3} µM for the other species).

1

2   **3.2. Fluxes of solutes**

3   Fluxes and total leaching of compounds were calculated for: the first four periods (P1–P4, 126

4   days) with a mean water flux of 2.65 L.d^{-1}; for the four periods after the addition of forest litter

5   (P5–P8, 138 days) with a mean water flux of 2.01 L.d^{-1}; and for the whole experiment (Tab. 1).

6   **Table 1:** Solute fluxes during the periods P1–P4 and P5–P8 (respectively before and after the addition
7   of organic litter). Water leachate volume was measured with a balance. Total compound leaching was
8   calculated by assuming that compound concentration in the leachate between two sampling operations
9   was equal to the concentration measured in the last sample. Water fluxes were calculated by dividing

22

the leachate volume by the total period duration and the elemental fluxes were calculated by dividing
the amount of compound leached during the period by the total period duration.

Period	P1-P4		P5-P8		Total	
Duration (day)	126		138		264	
Leachate volume (L)	334		278		612	
Water flux ($L.d^{-1}$)	2.65		2.01		2.32	
Major compounds	Flux ($mg.m^{-3}.d^{-1}$)	Total leaching ($g.m^{-3}$)	Flux ($mg.m^{-3}.d^{-1}$)	Total leaching ($g.m^{-3}$)	Flux ($mg.m^{-3}.d^{-1}$)	Total leaching ($g.m^{-3}$)
DOC	4,959.1	624.8	30,626.3	4,224.4	18,372.9	4,849.2
TA	4.1	0.5	2.5	0.4	3.3	0.9
Cl^-	203.9	25.7	87.9	12.1	143.3	37.8
Br^-	2.7	0.3	1.0	0.1	1.8	0.5
SO_4^{2-}	134.3	16.9	65.8	9.1	98.5	26.0
K^+	8.1	1.0	4.5	0.6	6.2	1.6
Na^+	11.4	1.4	5.9	0.8	8.6	2.3
Ca^{2+}	162.1	20.4	72.9	10.1	115.5	30.5
Mg^{2+}	12.8	1.6	6.4	0.9	9.4	2.5
Metals and arsenic						
Fe	1.90	0.24	3.03	0.42	2.49	0.66
Zn	374.85	47.23	260.63	35.63	315.16	83.18
Cu	0.75	0.10	0.34	0.05	0.54	0.14
As $_{total}$	14.46	1.82	12.56	1.73	13.47	3.55
As III-like	4.45	0.56	3.62	0.50	4.01	1.06
As V-like	11.47	1.45	7.61	1.05	9.45	2.50

During P6, 12 days have been excluded from calculation because the monitoring was stopped and no
water was input to the mesocosm.

After 276 days, the most leached compounds were DOC, Zn^{2+}, Cl^-, Ca^{2+}, SO_4^{2-} and, to a lesser

extent, As, Mg^{2+}, Na^+ and K^+. Among these compounds, Zn and As were the most mobile

metal(loid)s, with, respectively, total amounts of 83.18 and 3.55 $g.m^{-3}$ leached, with about 30%

of As III-like. Fluxes of DOC and Fe increased after the addition of OM, ranging from 4,959

to 30,626 $mg.m^{-3}.d^{-1}$ for DOC and 1.90 to 3.03 $mg.m^{-3}.d^{-1}$ for Fe. Between the first periods (P1-

P4) and the periods following the addition of organic litter (P5–P8), the majority of the other

compound fluxes were significantly halved, with the exception of As total flux which decreased

less after the addition of OM (from 14.46 to 12.56 $mg.m^{-3}.d^{-1}$).

3.3. Gas composition and carbon mineralization

Among all the gases analyzed (i.e. CO_2, O_2, H_2, N_2, N_2O, CO, CH_4 and BTEX) only CO_2, O_2, H_2, N_2 were detected in the atmosphere of the mesocosm during the experiment. CO_2 was the only gas for which concentrations varied (Fig. 4). The sum of the concentrations of CO_2, O_2, H_2 and N_2 was less than 100% because of the presence of water vapor in the mesocosm atmosphere. Prior to the addition of OM, the CO_2 concentrations seem to have been driven by the wet/dry periods, with higher concentration during the wet periods. CO_2 concentration was clearly affected by the addition of organic litter, with a strong increase from 0.137 to 0.556% during period P5. After this increase, the values dropped and stabilized at about 0.200%.

The rate of carbon mineralization in the mesocosm was evaluated at the end of periods P3, P4, P5, P6, P7 and P8 (Fig. 4). It was highest at the end of P5, the first period following the addition of OM, at 1.54 $\mu g\ CO_2\ g^{-1}$ dry mass.h^{-1}. No major difference was observed in the other periods, but rates were slightly higher at the end of dry periods (mean$_{(P3, P5, P7)}$ = 1.03 ± 0.27 $\mu g\ CO_2.g^{-1}$ dry mass.h^{-1}) than wet periods (mean$_{(P4, P6, P8)}$ = 0.67 ± 0.12 $\mu g\ CO_2.g^{-1}$ dry mass.h^{-1}), and were also higher after the addition of OM (mean$_{(P3-P4)}$ = 0.63 ± 0.08 $\mu g\ CO_2.g^{-1}$ dry mass.h^{-1}, mean$_{(P5-P8)}$ = 0.95 ± 0.24 $\mu g\ CO_2.g^{-1}$ dry mass.h^{-1}).

As volatilization from the mesocosm was evaluated at the end of each period. Dimethylarsine, quantified as dimethylarsinic acid (DMAA), was detected in traps for all periods. The mean rate of dimethylarsine volatilization was 1.65 ± 0.66 $ng.m^{-2}.d^{-1}$ for the first four periods and 5.83 ± 3.04 $ng.m^{-2}.d^{-1}$ after the addition of forest litter. The maximum rate of dimethylarsine volatilization was 16.13 $ng.m^{-2}.d^{-1}$ and corresponded to period P5. No other volatile As species was detected in the traps.

3.4. Leaching test

1 The contribution of soil and litter to the composition of water from the mesocosm experiment

2 was estimated by a leaching test with Mont Roucous water. The results for chemical parameters

3 and quantities of major ions and metal(loid) compounds are presented in Table 2.

4 **Table 2** Leaching test of the polluted soil (Soil) and the forest litter (OM).

	Soil			OM		
Chemical parameters						
pH	6.31	± 0.04	a	5.46	± 0.42	b
EC (μS.cm^{-1})	329.67	± 7.70	a	469.33	± 122.78	b
DOC (mg.kg^{-1})	333.45	± 3.95	a	3,085.17	± 120.78	b
Major ions (mg.kg^{-1})						
Na$^+$	23.05	± 0.05	a	42.74	± 0.87	b
K$^+$	9.00	± 0.03	a	110.74	± 0.22	b
Ca^{2+}	155.35	± 0.68	a	149.18	± 6.50	a
Mg^{2+}	9.91	± 0.01	a	23.71	± 0.80	b
Cl$^-$	24.78	± 0.01	a	15.81	± 1.23	a
Br$^-$	n.d.			3.60	± 0.04	
NO$_3^-$	34.57	± 0.25	a	183.49	± 6.48	b
SO$_4^{2-}$	144.57	± 0.13	a	43.60	± 1.89	b
PO$_4^{3-}$	n.d.			58.61	± 1.91	b
Meta(loid)s (mg.kg^{-1})						
As	47.75	± 0.10	a	344.02	± 4.07	b
Fe	< 0.1			10.91	± 0.58	
Zn	134.18	± 0.42	a	79.89	± 2.77	b
Pb	1.30	± 0.02	a	1.99	± 0.05	b
Cu	< 0.1			0.23	± 0.19	

5 Average values are expressed with their standard deviation (n=3). Values with different letters are
6 significantly different ($p < 0.05$, ANOVA Tukey-HSD)

7 The pH of leaching tests ranged from 6.31 in the "Soil" test to 5.46 in the "OM" test. EC and

8 DOC were significantly higher in the "OM" test. In the "Soil" leachate, Ca^{2+} and SO$_4^{2-}$ were

9 the most mobile ions, while Ca^{2+}, K$^+$ and NO$_3^-$ were the dominant ions in the "OM" leachate.

10 As indicated by EC, the "OM" leachate contained higher amounts of ions, especially Na$^+$, K$^+$,

11 Mg^{2+}, NO$_3^-$ and PO$_4^{3-}$. As, Fe, Pb and Cu were significantly more concentrated in leachate from

12 the forest litter than from contaminated soil, up to seven times for As. DPAA was identified in

13 the "Soil" leachate, with a concentration of 114 μg.L^{-1} (SM.2).

4. Discussion

4.1. Influence of saturation and OM on C and N cycles

Apart from the important concentration of metals and arsenic on the "Place-à-Gaz" site , this soil also contains a high amount of organic carbon (up to 250 g/kg, Thouin *et al.*, 2016). As demonstrated in the previous study (Thouin *et al.*, 2016), two types of organic matter with very different biodegradabilities are present on the site: low degradable organic matter, inherited from the burning of firewood used during the destruction of ammunition (charcoal); and more biodegradable organic matter that comes from the forest litter. Charcoal accounts for most of the organic matter in the central part of the site. Wildfire-formed charcoals have the potential to greatly enhance soil fertility by enhancing N cycling (Berglund *et al.*, 2004), and to provide habitat for microbial life (Pietikainen *et al.*, 2000). However, the "Place-à-Gaz" site has been characterized by a lack of vegetation in its central part for almost a century. It is therefore obvious that charcoals, both bearing and mixed with high amounts of contaminants, have not promoted growth of vegetation on the site. Charcoals' stability and resistance to microbial degradation make them important long-term carbon sinks (Schmidt and Noack, 2000), meaning that most of the organic matter on the site is not bioavailable for the growth of microorganisms and vegetation. In the surrounding areas, close to the forest, three species have colonized the contaminated soil: a moss *Pohlia nutans* (Hedw.), a lichen *Cladonia fimbriata* (L.), and an herbaceous species *Holcus lanatus* (L.). The input of forest litter, which provides bioavailable nutrients, was certainly the cause of plants establishing themselves and then also influenced the site's carbon cycle.

The mesocosm experiment described here studied the modification of the carbon cycle induced by the input of oak forest litter. DOC concentrations in the mesocosm experiment were always higher than the common range of DOC concentration in soil water (Boyer *et al.*, 1996, Clarke

et al., 2005). A major part of the DOC in the mesocosm may be derived from the burned organic matter that might not have been entirely mineralized. Similar DOC concentrations, ranging from 25 to 7500 mM, were reported in leachates from disposal sites which contained municipal solid waste incineration residues (Seo *et al*., 2007). Here, the addition of forest litter induced a significant increase in DOC concentration in the soil water (Fig. 4) and a very high flux of DOC during the periods following the input (Tab. 2). The results of the leaching experiment – showing a significantly higher amount of organic carbon leached from the forest litter than from the contaminated soil (Tab. 4) – underpin the impact of forest litter on DOC content in the soil water. DOC is the primary carbon source for heterotrophic bacteria in soils (Metting, 1993, Horemans *et al*., 2013), so the increase in the carbon mineralization rate in the mesocosm after the addition of organic litter (Fig. 3) seems to be directly linked to the biodegradation activity of microorganisms. The increase of CO_2 concentration in the mesocosm atmosphere during the period P5, from 0.137% to 0.556% (Fig. 3), is another consequence of this high carbon mineralization activity.

The mineralization of organic matter by microbial metabolism is conditioned by the accessibility of terminal electron acceptors (TEA). Oxygen is the most efficient TEA available in the environment, and carbon mineralization consumes oxygen. Microbial respiration impacted the dissolved oxygen content and indirectly the redox potential, which decreased after the addition of organic matter (P6-P8). The reductive process, and hence the Eh decrease, are generally driven by the consumption/oxidation of DOC coupled with the reduction of the successive TEA's by the bacterial community (Weber et al., 2006). Here, dissolved oxygen also appeared to be determined by depth and by water saturation, even if it was not visible at level H3, alternately saturated and unsaturated.

Soil moisture and oxygen availability can influence the nitrogen cycle (Silver *et al*., 2001; Rubol *et al*., 2013). Cycles of nitrate disappearance at level H3 may be interpreted as

denitrification and demonstrate at least that the nitrogen cycle was strongly affected by water saturation, the Eh value in level H3 being close to the limit allowing denitrification (713 mV, Weber et al., 2006). During denitrification, nitrate and nitrite are reduced to N_2 gas by heterotrophic denitrifiers in the presence of OM as electron donor. Even though no significant variation of N_2 was observed in the atmosphere, the production of nitrite during each wet period and the variation of alkalinity can be interpreted as the result of denitrification. Nevertheless other metabolic pathways could be responsible of the observed nitrate decrease, namely dissimilatory nitrate reduction to ammonium (DNRA). DNRA activity is favored by temperatures superior to 10°C and is less sensitive than denitrification to variations of nitrate concentrations as it can be sustained at lower concentrations (Roberts et al., 2014). Additionally, DNRA activity is also less affected by the inhibitory effects of O_2 (and equilibrium between denitrification and DNRA seems to be mainly driven by bioavailable carbon (Fazzolari *et al.*, 1998; Hardison et al., 2015). The large amounts of OM that have been initially quantified and subsequently added to the experiments could plead in favor of DNRA prevalence; nevertheless the bioavailability of this carbon source for the reduction of nitrate is still unknown. Moreover, DNRA may outcompete denitrification with other sources of electron donors, namely Fe II and sulfide (Roberts et al., 2014), but the present experiment displayed Eh and DOs that were not compatible with the presence of such reduced species (i.e. DO > 50 µM and Eh > 250 mV). The amounts of ammonium detected during the experiment in the lower part of the mesocosm could be attributed to ammonification processes or DNRA. Nevertheless, in the saturated level (H4) and in the leachate, the rapid disappearance of nitrate concomitant with the appearance of nitrite and the increase in ammonium concentration seem more logically linked to DNRA activity. The fact that these quantities (few µM) does not match with the loss of nitrate (few hundreds µM) is however not a proof of low DNRA activity because ammonium can possibly be consumed by other metabolic pathways. For instance, it can be assimilated to

form biomass or oxidized into N_2 by Anammox and/or Feammox dissimilative processes with nitrite and Fe III respectively (Francis et al., 2007). The coupling of DNRA and Anammox metabolic pathways is known to be difficult to discriminate with denitrification processes in terms of mass balance and is possibly responsible of frequent false interpretations in that matter (Francis et al., 2007). As a result, it appears difficult to state which of these two metabolic pathways was predominant in the mesocosm during our study.

The increase of nitrate concentration during dry periods at level H3 may have been the result of nitrification thanks to ammonium production from DNRA providing a source of NH_4^+ for nitrifying bacteria (Burgin and Hamilton, 2007). However, the small amount of NH_4^+ in this level during the saturation periods, and the absence of nitrite simultaneously with the increase in nitrates during the dry periods, suggested that nitrification was not the main process inducing the increase of nitrate when soil was desaturated. The soil water from the surface of the mesocosm was rich in NO_3^- and the transport of nitrate down towards the H3 level may explain this phenomenon.

Some nitroaromatic compounds, and particularly 1,3-Dinitrobenzene, had been detected previously on the "Place-à-Gaz" site (Bausinger *et al*., 2007), and in another former World War I ammunition destruction facility (Bausinger and Preuβ, 2005). Nitroaromatic compounds on this site (range 1 mg.kg^{-1}) were less concentrated than soil from ammunition plants (range 1 g.kg^{-1}) resulting from the recent incineration of explosives (Kalderis *et al*., 2011). Even after more than 80 years, the nitroaromatic concentrations in soil from the "Place-à-Gaz" highlight the persistence of nitroaromatic explosives and their metabolites in the environment. However, no nitroaromatic compound was detected in the soil or solution water of the mesocosm (SM.2 and SM.3). This observation may be caused to the complete degradation of nitroaromatic compounds. Several studies have shown that microbial aerobic degradation of nitroaromatic compounds releases nitrogen as nitrite into the environment (Marvin-Sikkema and de Bont,

1 1994; Spain, 1995). The total degradation of nitroaromatic compounds to inorganic forms

2 was potentially an important source of nitrogen in this type of site. The organic litter was also

3 rich in leachable NO_3^- (Tab. 2), arising mainly from the decomposition of plant OM. The

4 increase in NO_3^- in level H2 following the addition of organic matter highlighted the supply of

5 NO_3^- by the forest litter.

6 **4.2. Behavior of metals and metalloids, and possible evolution of their mobility in the**

7 **context of changing site conditions**

8 In line with the *in situ* observations of the "Place-à-Gaz" soil (Bausinger *et al*., 2007; Thouin

9 *et al*., 2016), Zn and As were the most mobile metal(oid)s in the mesocosm. Zn concentration

10 in the soil water showed a time related evolution with a delay in maximum concentration with

11 depth. This particular evolution, also observed for Ca^{2+} and Mg^{2+} (SM.5) concentrations and

12 EC, can be attributed to the leaching of Zn which was mobile in the pH range of 5–6. The initial

13 concentrations of Zn at each depth and in the leachate were fairly similar and mobilization of

14 Zn at the beginning of the experiment was thus comparable throughout the soil profile.

15 However, after several periods, Zn mobility was greater in the saturated soil. The amount of Zn

16 leached in saturated soils is commonly explained by a pH decreased cationic exchange capacity

17 releasing the adsorbed Zn. However, in this case, the stability of pH during the experiment and

18 throughout the soil profile suggests that desorption of easily exchangeable Zn is not the only

19 phenomenon driving Zn mobility in water. Previous studies (Bausinger *et al*., 2007, Thouin *et*

20 *al*., 2016) showed that the main carrier of Zn was an amorphous material that also contained

21 large amounts of As, Pb, Cu and Fe. The dissolution of this amorphous material, whose

22 conditions of stability are unknown, may release enough Zn to explain the increase in Zn

23 concentration in the saturated soil. However, the other metals present in this amorphous phase

24 were not very abundant in the solution.

30

The pH of the soil water may explain the low solubility of Pb and Cu, as Bausinger *et al*. (2007)

have shown that Pb and Cu were not mobile in the soil of the site at pH 5–6. Cu and Pb were

probably adsorbed on soil grain surfaces or precipitated with the other ions present in solution.

The oxidation-reduction potential (Eh) and pH conditions of the experiment were favorable to

the precipitation of ferric oxides like hematite or magnetite or hydrous ferric oxides (HFO) like

ferrihydrite or goethite. The precipitation of HFO allows the sorption of Cu and Pb onto their

surface (Swallow *et al*., 1980; Morin *et al*., 2001), and would explain their low solubility. Fe

seemed to be the metal most impacted by dry/wet cycles, but the trend was not very clear even

if the behavior of Fe in the top soil seems to be different from that in the saturated levels. In

addition, the Fe concentration trends showed that Fe mobility decreased significantly in the

unsaturated soil and increased significantly in soil levels that were alternately or permanently

saturated. The addition of organic litter enhanced these trends and DOC seemed to have a

greater impact on Fe mobility than dry/wet cycles. Moreover, it was probable that iron analyzed

in soil water and in the leachate was particulate or colloidal. The study of the colloidal fraction

and the iron speciation could help to explain the behavior of iron in this specific polluted

material.

Together with Zn, As was the major metal(loid) present in the soil water, with concentrations

up to 800 times higher than the maximum level of $10 \ \mu g \ L^{-1}$ recommended by the WHO (2011).

However, As behaved differently from Zn, with higher concentration at the top of the mesocosm

and immobilization with increasing depth. Previous studies describing As behavior during

redox oscillation (Parsons *et al*., 2013, Couture *et al*., 2015) have shown that the successive

cycles of oxidizing and reducing conditions (between -300 and +500 mV) affect As mobility in

relation with As speciation and sorption onto HFO. During oxidizing cycles, As is strongly

associated with HFO; during reducing periods, the combination of reduction of Fe oxides and

microbial reduction of As V to As III raises As solubility (Couture *et al*., 2015). Under the

conditions of this experiment, dry/wet cycling did not induce reducing conditions, even in the permanently saturated level. Moreover, As V was always the major As species in solution and presented an evolution similar to total As. However, the decrease in As V concentration with depth could be induced by the precipitation of HFO or iron oxide from Fe leached by the dissolution of the amorphous phase in the saturated level, as As V is more readily adsorbed onto HFO than As III at pH 5–6 (Dixit and Hering, 2003). Between H4 and L, As V concentration decreased by about 50% (Fig. 6). This very large decrease may be linked to the precipitation of HFO or the growth of a biofilm from the soil, perhaps on the geotextile membrane. The precipitation of secondary arsenates as an explanation for the immobilization of As V in solution cannot be excluded.

As III seems to be affected by the wet/dry cycles: the higher As III concentration at the end of wet periods at all levels (Fig. 7) was probably linked to less oxygenated water and decreased ORP. Previous studies demonstrated the importance of iron and As V reduction by microorganisms on the mobility of As in groundwaters (Islam, 2005). Also, the proportion of As III in water increased with depth, supporting the fact that As III behavior may be by soil saturation. Biological As III oxidation activity had been detected previously in the soil of the "Place-à-Gaz" site under unsaturated conditions (Thouin *et al*., 2016), thus bacteria involved in the cycle of arsenic were present in the mesocosm. The hypothesis of microbial reduction of As V cannot be ruled out, whereas desorption of As III might be involved in the observed evolution of dissolved As speciation (Tufano *et al*., 2008).

The excess of DOC after the addition of bioavailable OM promoted microbial respiration and Eh drop, but also enhanced Fe mobility. This process should have enhanced As mobility, but in fact immobilization of As, mainly as As V, was observed over the different depths. The addition of fresh organic matter may have contributed by providing adsorption sites enough to trap some As V. It also appears that more dimethylarsine was produced after the input of OM.

However, despite the important concentration of As in soil, arsine volatilization were lower than As fluxes observed earlier in wetland (160-540 $ng.m^{-2}.d^{-1}$; Vriens *et al.*, 2014) paddy soil (Bangladeshi paddy soil 65 $ng.m^{-2}.d^{-1}$, Spain paddy soil 12 $ng.m^{-2}.d^{-1}$; Mestrot *et al.*, 2011) or amended mine soil (Moreno-Jiménez *et al.*, 2013). The volatilization of arsines and by As methylation seems to be limited by the sub-oxic conditions and was too low to explain As decrease in solution. However, increase of dimethylarsine flux after OM addition confirmed the influence of OM on the activity of As transforming microbes in this soil (Huang *et al.*, 2011). The addition of OM also induced an increase in As III concentration in the saturated soil (Fig. 6 and Fig. 7). The organic carbon concentration influences the rate of microbial As III oxidation in soils, a decrease in oxidation rate being observed beyond 0.08 $g.L^{-1}$ of organic carbon (Lescure *et al.*, 2016).

Among the soluble As species, DPAA (SM.2) and three unidentified species were also detected (Fig. 7). The sum of these compounds and As III and As V was approximately equal to total As, indicating that no other main As species was present. It also appears that the unidentified species were not in ionic form, since the sum of these species and As III (Fig. 7) was similar to the As III-like species concentration given by anionic resin separation (Fig. 6). DPAA, the hydrolysis product of the chemical warfare agent (Clark I and Clark II), was detected in low concentration at the outlet of the mesocosm. This compound was identified in water from this contaminated soil for the first time, since aromatic arsenicals had not been detected previously on the site (Bausinger *et al.*, 2007). The bacterial degradation pathway of DPAA in soil may produce phenylarsonic acid (PAA; Harada *et al.*, 2010) or phenylarsine oxide (PAO) in less oxidizing conditions (Daus *et al.*, 2010). DPAA was not detected in the deeper zones of groundwater contaminated by a former ammunition deposit and chemical warfare agent filling station (Daus *et al.*, 2010). This absence was concomitant with occurrence of PAO and with As III increase, while PAA was detected all along the depth profile. In our experiment, with similar

Eh and pH conditions, the unidentified species 1, which was very stable independently of the changing conditions, might have been attributed to PAA, and unidentified species 2, which only appeared in saturated conditions, to PAO. The three unidentified species could therefore be metabolites of DPAA, or may have resulted from the oxidation of Clark I and II during combustion with a more complex degradation pathway. Further investigation is required to identify these compounds and understand their origin.

With time, water soluble compounds, including metals and As, will be progressively leached from the soil profile. The 8-months mesocosm experiment represented about one year of precipitation on the "Place-à-Gaz" site with a succession of dry and wet periods simulating seasonal variations. If the fluxes leached from the soil during the mesocosm experiment are considered as being in the same range as on-site horizontal leaching fluxes, since the year 1928 (when the shells were destroyed), several tons of Zn and several tens of kilograms of As could have been leached from the site (containing about 1500 m^3 i.e. 3000 tons of contaminated material, personal communication) by runoff to the surrounding surface environment. The high concentration of soluble As and metals leached from the forest litter sampled from outside of the site attested to the important runoff of pollutants. The high concentration of soluble As and metals in the top layer of forest soil, and principally in the litter and humic horizon, can be very problematic for wildlife. Results also suggest that this type of site may provide a stock of As from which leaching will continue for several thousand years.

5. Conclusion

For nearly one hundred years, the highly polluted site known as "Place-à-Gaz" has been submitted to: (i) water saturation during rainfall events, inducing the transfer of pollutants to the surrounding forest environment via surface runoff; and (ii) natural deposition of oak litter. In the mesocosm experiment described above, the soil was submitted to dry/wet cycles and to

the addition of organic litter from the site in order to evaluate the influence of soil saturation

levels and of bioavailable OM on the biogeocycles of C, N and metal(oid)s.

Organic carbon present on the site was mainly charcoal and did not provide bioavailable

nutrients to restore the soil's biological functions. The addition of organic litter at the top of the

contaminated soil increased microbial activity. The nitrogen cycle was clearly affected by the

dry/wet cycles, with microbial denitrification occurring in saturated conditions. Nitroaromatic

compounds and cyano-arsines were present as sources of nitrogen in the chemical shells

subjected to burning, and the results have highlighted the persistent nature of nitrogen on this

type of site.

As and Zn were the most mobile metal(oid)s but behaved differently as the experiment

progressed. Zinc concentration in soil water increased with depth and was not affected by the

dry/wet cycles nor by the addition of organic litter; arsenic was more concentrated in the

unsaturated soil. Concentration of As V, the major As species in solution, decreased with depth,

while the proportion of As III increased in saturated conditions and with increased

bioavailability of OM. At the end of the experiment, the soil released less As but with a greater

proportion of more toxic As III. Four other As species were also detected in solution in

significant concentrations: DPAA, the hydrolysis product of the warfare agents, and three

unidentified species. Low concentration of Fe, Cu and Pb in solution was caused by the

precipitation of iron oxide-hydroxide and/or the low solubility of Cu and Pb in these pH

conditions.

The experiment underlined the high potential for Zn and As mobilization all around the site by

surface water runoff, but also showed that the deposition of forest litter contributes to the

immobilization of some As. However, the proportion of As III, the most toxic As species, is

also enhanced. Furthermore, progressive growth of vegetation on the site, enabled by the

bioavailable organic matter from litter, may modify the behavior of contaminants. To complete understanding of the fate of inorganic pollutants along with the evolution of environmental conditions on this singular site, the effects of the rhizosphere should be investigated. The instrumented mesocosm used in the present study allowed studying the site-observed phenomena at an intermediate scale between the field and a laboratory microcosm. The parameters that could be controlled (saturation level) and the quantities of collected data proved that this mesocosm can be a convenient experimental device to study the influence of environmental events on the behavior of contaminants.

Acknowledgments

References

Aller, R. C. (1994). Bioturbation and remineralization of sedimentary organic matter: effects of redox oscillation. Chemical Geology *114*, 331–345.
DOI: 10.1016/0009-2541(94)90062-0

Anderson, T.R., Goodale, C.L., Groffman, P.M., and Walter, M.T. (2014). Assessing denitrification from seasonally saturated soils in an agricultural landscape: A farm-scale mass-balance approach. Agriculture, Ecosystems & Environment *189*, 60–69.
DOI: 10.1016/j.agee.2014.03.026

Bada K, Arao T., Maejima, Y., Watanabe, E., Eun, H., and Ishizaka, M. (2008). Arsenic speciation in rice and soil containing related compounds of chemical warfare agents. Analytical Chemistry *80,* 5768–5775.
DOI: 10.1021/ac8002984

Banks, M.K., Clennan, C., Dodd, W., and Rice, C. (1999). Variations in microbial activity due to fluctuations in soil water content at the water table interface. Journal of Environmental Science and Health *34*, 479-505.
DOI: 10.1080/10934529909376849

Bausinger, T., and Preuß, J. (2005). Environmental remnants of the First World War: Soil contamination of a burning ground for arsenical ammunition. Bulletin of Environmental Contamination and Toxicology *74*, 1045–1053.
DOI: 10.1007/s00128-005-0686-z

Bausinger, T., Bonnaire, E., and Preuß, J. (2007). Exposure assessment of a burning ground for chemical ammunition on the Great War battlefields of Verdun. Science of The Total Environment *382*, 259–271.
DOI: 10.1016/j.scitotenv.2007.04.029

Bauer, M., and Blodau, C. (2006). Mobilization of arsenic by dissolved organic matter from iron oxides, soils and sediments. Science of the Total Environment *354*, 179-190.
DOI: 10.1016/j.scitotenv.2005.01.027

Berglund, L.M., DeLuca, T.H., and Zackrisson, O. (2004). Activated carbon amendments to soil alters nitrification rates in Scots pine forests. Soil Biology and Biochemistry *36*, 2067–2073. Ecological Modelling *86*, 183-188.
DOI: 10.1016/j.soilbio.2004.06.005

Blodau, C., and Moore, T. (2003). Experimental response of peatland carbon dynamics to a water table fluctuation. Aquatic Sciences *65*, 47–62.
DOI: 10.1007/s000270300004

Boyer, E.W., Hornberger, G.M., Bencala, K.E., and McKnight, D. (1996). Overview of a simple model describing variation of dissolved organic carbon in an upland catchment. Ecological Modelling *86*, 183–188.
DOI: 10.1016/0304-3800(95)00049-6

Burgin, A.J., and Hamilton, S.K. (2007). Have we overemphasized the role of denitrification in aquatic ecosystems? A review of nitrate removal pathways. Frontiers in Ecology and the Environment *5*, 89–96.
DOI: 10.1890/1540-9295(2007)5[89:HWOTRO]2.0.CO;2

Certini, G., Scalenghe, R., and Woods, W. I. (2013). The impact of warfare on the soil environment. Earth-Science Review *127*, 1-15.
DOI: 10.1016/j.earscirev.2013.08.009

Clarke N., Rosberg I., Aamlid D. (2005) Concentrations of dissolved organic carbon along an altitudinal gradient from Norway spruce forest to the mountain birch/alpine ecotone in Norway. Boreal Environment Research *10*, 181-189.

Couture, R.-M., Charlet, L., Markelova, E., Madé, B., and Parsons, C.T. (2015). On–off mobilization of contaminants in soils during redox oscillations. Environmental Science & Technology *49*, 3015–3023.
DOI: 10.1021/es5061879

Daus, B., Hempel, M., Wennrich, R., and Weiss, H. (2010). Concentrations and speciation of arsenic in groundwater polluted by warfare agents. Environmental Pollution *158*, 3439–3444.
DOI: 10.1016/j.envpol.2010.06.029

DeAngelis, K.M., Silver, W.L., Thompson, A.W., and Firestone, M.K. (2010). Microbial communities acclimate to recurring changes in soil redox potential status. Environmental Microbiology *12*, 3137–3149.
DOI: 10.1111/j.1462-2920.2010.02286.x

Dixit, S., and Hering, J.G. (2003). Comparison of Arsenic(V) and Arsenic(III) Sorption onto Iron Oxide Minerals: Implications for Arsenic Mobility. Environmental Science & Technology *37*, 4182–4189.
DOI: 10.1021/es030309t

Dobran, S., and Zagury, G.,J. (2006). Arsenic speciation and mobilization in CCA-contaminated soils: Influence of organic matter content. Science of the Total Environment *364*, 239-250.
DOI: 10.1016/j.scitotenv.2005.06.006

Dutta, T., Carles-Brangarí, A., Fernàndez-Garcia, D., Rubol, S., Tirado-Conde, J., and Sanchez-Vila, X. (2015). Vadose zone oxygen (O2) dynamics during drying and wetting cycles: An artificial recharge laboratory experiment. Journal of Hydrology *527*, 151–159.
DOI: 10.1016/j.jhydrol.2015.04.048

Fazzolari, É., Nicolardot, B., and Germon, J.C. (1998). Simultaneous effects of increasing levels of glucose and oxygen partial pressures on denitrification and dissimilatory nitrate reduction to ammonium in repacked soil cores. European Journal of Soil Biology *34*, 47–52.
DOI: 10.1016/S1164-5563(99)80006-5

Francis, C.A., Beman, J.M., and Kuypers, M. M. (2007). New processes and players in the nitrogen cycle: the microbial ecology of anaerobic and archaeal ammonia oxidation. The ISME journal *1*(1), 19-27.

DOI: 10.1038/ismej.2007.8

Gadd, G.M. (2004). Microbial influence on metal mobility and application for bioremediation. Geoderma *122,* 109–119.
DOI: 10.1016/j.geoderma.2004.01.002

Harada, N., Takagi, K., Baba, K., Fujii, K., and Iwasaki, A. (2010). Biodegradation of diphenylarsinic acid to arsenic acid by novel soil bacteria isolated from contaminated soil. Biodegradation *21*, 491–499.
DOI: 10.1007/s10532-009-9318-3

Hardison, A.K., Algar, C.K., Giblin, A.E., and Rich, J. J. (2015). Influence of organic carbon and nitrate loading on partitioning between dissimilatory nitrate reduction to ammonium (DNRA) and N 2 production. Geochimica et Cosmochimica Acta *164*, 146-160.
DOI: 10.1016/j.gca.2015.04.049

Hirsch, R.M., Slack, J.R., and Smith, R.A. (1982). Techniques of trend analysis for monthly water quality data. Water Resources Research *18*, 107–121.
DOI: 10.1029/WR018i001p00107

Hirsch, R.M., and Slack, J.R. (1984). A nonparametric trend test for seasonal data with serial dependence. Water Resources Research *20*, 727–732.
DOI: 10.1029/WR020i006p00727

Horemans, B., Vandermaesen, J., Smolders, E., and Springael, D. (2013). Cooperative dissolved organic carbon assimilation by a linuron-degrading bacterial consortium. FEMS Microbiology Ecology *84*, 35–46.
DOI: 10.1111/1574-6941.12036

Howard, D.M., and Howard, P.J.A. (1993). Relationships between CO2 evolution, moisture content and temperature for a range of soil types. Soil Biology and Biochemistry *25*, 1537–1546.
DOI: 10.1016/0038-0717(93)90008-Y

Hua, L., Wu, W., Liu, Y., McBride, M.B., and Chen, Y. (2009). Reduction of nitrogen loss and Cu and Zn mobility during sludge composting with bamboo charcoal amendment. Environmental Science and Pollution Research *16*, 1–9.
DOI: 10.1007/s11356-008-0041-0

Huang, J.-H., Hu, K.-N., and Decker, B. (2011). Organic arsenic in the soil environment: speciation, occurrence, transformation, and adsorption behavior. Water Air Soil Pollut *219*, 401–415.
DOI : 10.1007/s11270-010-0716-2

Huang, H., Jia, Y., Sun, G.-X., and Zhu, Y.-G. (2012). Arsenic speciation and volatilization from flooded paddy soils amended with different organic matters. Environmental Science & Technology *46*, 2163–2168.
DOI: 10.1021/es203635s

Huot, H., Séré, G., Charbonnier, P., Simonnot, M.-O., and Morel, J.L. (2015). Lysimeter monitoring as assessment of the potential for revegetation to manage former iron industry settling ponds. Science of The Total Environment *526*, 29–40.
DOI: 10.1016/j.scitotenv.2015.04.025

Islam, F.S., Gault, A.G., Boothman, C., Polya, D.A., Charnock, J.M., Chatterjee, D., and Lloyd, J.R. (2004). Role of metal-reducing bacteria in arsenic release from Bengal delta sediments. Nature *430*, 68–71.
DOI: 10.1038/nature02638

ISO 11916-1. (2013). Soil quality – Determination of selected explosive compounds – Part 1: Method using high performance liquid chromatography (HPLC) with ultraviolet detection, Geneva, Switzerland: International Organization for Standardization.

Joos, A., Knackmuss, H. J., and Spyra, W. (2008). Natürliche schadstoffminderungsprozesse bei sprengstofftypischen verbindungen; prozessverständnis, methoden, Referenzstandorte, Empfehlungen und Hinweise zur Einzelfallbearbeitung, Leitfaden. KORA-TV 5, Rüstungsaltlasten.

Kalderis, D., Juhasz, A.L., Boopathy, R., and Comfort, S. (2011). Soils contaminated with explosives: Environmental fate and evaluation of state-of-the-art remediation processes (IUPAC Technical Report). Pure and Applied Chemistry *83*, 1407–1484.
DOI: 10.1351/PAC-REP-10-01-05

Kendall M. G., Rank Correlation Methods, Griffin, London (1948).

Kim, M.-J. (2001). Separation of Inorganic Arsenic Species in Groundwater Using Ion Exchange Method. Bulletin of Environmental Contamination and Toxicology *67*, 0046–0051.
DOI: 10.1007/s00128-001-0089-8

Kowalenko, C.G., Ivarson, K.C., Cameron, D.R. (1978). Effect of moisture content, temperature and nitrogen fertilization on carbon dioxide evolution from field soils. Soil Biology and Biochemistry *10*, 417-423.
DOI: 10.1016/0038-0717(78)90068-8

Kumpiene, J., Ragnvaldsson, D., Lövgren, L., Tesfalidet, S., Gustavsson, B., Lättström, A., Leffler, P., and Maurice, C. (2009). Impact of water saturation level on arsenic and metal mobility in the Fe-amended soil. Chemosphere *74*, 206–215.
DOI: 10.1016/j.chemosphere.2008.09.068

Lawrence, M.J., Stemberger, H.L.J., Zolderdo, A.J., Struthers, D.P., and Cooke, S.J. (2015). The effects of modern war and military activities on biodiversity and the environment. Environmental Reviews *23*, 443–460.
DOI: 10.1139/er-2015-0039

Lescure, T., Moreau, J., Charles, C., Ben Ali Saanda, T., Thouin, H., Pillas, N., Bauda, P., Lamy, I., and Battaglia-Brunet, F. (2015). Influence of organic matters on AsIII oxidation by the microflora of polluted soils. Environmental Geochemistry and Health *38*, 911–925.
DOI: 10.1007/s10653-015-9771-3

Linn, D.M., and Doran, J.W. (1984). Effect of water-filled pore space on carbon dioxide and nitrous oxide production in tilled and nontilled soils. Soil Sci. Soc. Am. J. *48*, 1667–1672.

Mann H.B. (1945). Nonparametric tests against trend, Econometrica *13*, 245–259.

Marvin-Sikkema, F.D., and de Bont, J.A.M. (1994). Degradation of nitroaromatic compounds by microorganisms. Applied Microbiology and Biotechnology *42*, 499–507.
DOI: 10.1007/BF00173912

Moreno-Jiménez, E., Clemente, R., Mestrot, A., and Meharg, A.A. (2013). Arsenic and selenium mobilisation from organic matter treated mine spoil with and without inorganic fertilisation. Environmental Pollution *173*, 238–244.
DOI: 10.1016/j.envpol.2012.10.017

Mestrot, A., Uroic, M.K., Plantevin, T., Islam, M.R., Krupp, E.M., Feldmann, J., and Meharg, A.A. (2009). Quantitative and qualitative trapping of arsines deployed to assess loss of volatile arsenic from paddy Soil. Environmental Science & Technology *43*, 8270–8275.
DOI: 10.1021/es9018755

Mestrot, A., Feldmann, J., Krupp, E.M., Hossain, M.S., Roman-Ross, G., and Meharg, A.A. (2011). Field Fluxes and Speciation of Arsines Emanating from Soils. Environmental Science & Technology *45*, 1798–1804.
DOI: 10.1021/es103463d

Metting, F. B. (ed). (1993). Structure and physiological ecology of soil microbial communities. Soil Microbial Ecology - Application in Agricultural and Environmental Management. pp. 3–24. Marcel Dekker, New York.

Moreno-Jiménez, E., Clemente, R., Mestrot, A., and Meharg, A.A. (2013). Arsenic and selenium mobilisation from organic matter treated mine spoil with and without inorganic fertilisation. Environmental Pollution *173*, 238–244.
DOI : 10.1016/j.envpol.2012.10.017

Morin, G., Juillot, F., Ildefonse, P., Calas, G., Samama, J.-C., Chevallier, P., and Brown, G.E. (2001). Mineralogy of lead in a soil developed on a Pb-mineralized sandstone (Largentière, France). American Mineralogist *86*, 92–104.
DOI: 10.2138/am-2001-0110

Onken, B.M., and Adriano, D.C. (1997). Arsenic availability in soil with time under saturated and subsaturated conditions. Soil Science Society of America Journal *61*, 746.
DOI: 10.2136/sssaj1997.03615995006100030007x

Park, J.H., Lamb, D., Paneerselvam, P., Choppala, G., Bolan, N., and Chung, J.-W. (2011). Role of organic amendments on enhanced bioremediation of heavy metal(loid) contaminated soils. Journal of Hazardous Materials *185*, 549–574.
DOI: 10.1016/j.jhazmat.2010.09.082

Parsons, C.T., Couture, R.-M., Omoregie, E.O., Bardelli, F., Greneche, J.-M., Roman-Ross, G., and Charlet, L. (2013). The impact of oscillating redox conditions: Arsenic immobilisation in contaminated calcareous floodplain soils. Environmental Pollution *178*, 254–263.
DOI : 10.1016/j.envpol.2013.02.028

Pietikainen, J., Kiikkila, O., and Fritze, H. (2000). Charcoal as a habitat for microbes and its effect on the microbial community of the underlying humus. Oikos *89*, 231–242.
DOI: 10.1034/j.1600-0706.2000.890203.x

Rey, A., Petsikos, C., Jarvis, P.G., and Grace, J. (2005). Effect of temperature and moisture on rates of carbon mineralization in a Mediterranean oak forest soil under controlled and field conditions. European Journal of Soil Science *56*, 589–599.
DOI: 10.1111/j.1365-2389.2004.00699.x

Roberts, K.L., Kessler, A.J., Grace, M.R., and Cook, P.L. (2014). Increased rates of dissimilatory nitrate reduction to ammonium (DNRA) under oxic conditions in a periodically hypoxic estuary. Geochimica et Cosmochimica Acta *133*, 313-324.
DOI: 10.1016/j.gca.2014.02.042

Rodrigo, A. Recous S., Neel, C., and Mary, B. (1997) Modelling temperature and moisture effects on C–N transformations in soils: comparison of nine models. Ecological Modelling *102,* 325–339.
DOI: 10.1016/S0304-3800(97)00067-7

Rubol, S., Silver, W.L., and Bellin, A. (2012). Hydrologic control on redox and nitrogen dynamics in a peatland soil. Science of The Total Environment *432*, 37–46.
DOI : 10.1016/j.scitotenv.2012.05.073

Rubol, S., Manzoni, S., Bellin, A., and Porporato, A. (2013). Modeling soil moisture and oxygen effects on soil biogeochemical cycles including dissimilatory nitrate reduction to ammonium (DNRA). Advances in Water Resources *62*, *Part A*, 106–124.
DOI: 10.1016/j.advwatres.2013.09.016

Schmidt, M.W.I., and Noack, A.G. (2000). Black carbon in soils and sediments: Analysis, distribution, implications, and current challenges. Global Biogeochemical Cycles *14*, 777–793.
DOI: 10.1029/1999GB001208

Schulz-Zunkel, C., Rinklebe, J., Hans-Rudolf, B., (2015). Trace element release patterns from Three floodplain soils under simulated oxidized–reduced cycles. Ecological Engineering *83*, 485-495.
DOI: 10.1016/j.ecoleng.2015.05.028

Seo D.-J., Kim Y-Ji, Ham S.-Y., and Lee D.-H. (2007) Characterization of dissolved organic matter in leachate discharged from final disposal sites which contained municipal solid waste incineration residues. Journal of Hazardous Materials *148,* 679–692.
DOI: 10.1016/j.jhazmat.2007.03.027

Silver, W.L., Lugo, A.E., and Keller, M. (1999). Soil oxygen availability and biogeochemistry along rainfall and topographic gradients in upland wet tropical forest soils. Biogeochemistry *44*, 301–328.
DOI: 10.1007/BF00996995

Silver, W.L., Herman, D.J., and Firestone, M.K., (2001) Dissimilatory nitrate reduction to ammonium in upland tropical forest soils. Ecology *82*, 2410–2416.
DOI: 10.1890/0012-9658(2001)082[2410:DNRTAI]2.0.CO;2

Spain, J.C. (1995). Bacterial degradation of nitroaromatic compounds under aerobic conditions. In Biodegradation of Nitroaromatic Compounds, J.C. Spain, ed. (Boston, MA: Springer US), pp. 19–35.

Swallow, K.C., Hume, D.N., and Morel, F.M.M. (1980). Sorption of copper and lead by hydrous ferric oxide. Environmental Science & Technology *14*, 1326–1331.
DOI: 10.1021/es60171a003

Thouin, H., Le Forestier, L., Gautret, P., Hube, D., Laperche, V., Dupraz, S., and Battaglia-Brunet, F. (2016). Characterization and mobility of arsenic and heavy metals in soils polluted by the destruction of arsenic-containing shells from the Great War. Science of The Total Environment *550*, 658–669.
DOI: 10.1016/j.scitotenv.2016.01.111

Tufano, K., Reyes, C, Saltikov, C.W., and Fendorf, S.. (2008). Reductive processes controlling arsenic retention: revealing the relative importance of iron and arsenic reduction. Environmental Science & Technology *42*, 8283-9
DOI: 10.1021/es801059s

Vriens, B., Lenz, M., Charlet, L., Berg, M., and Winkel, L.H.E. (2014). Natural wetland emissions of methylated trace elements. Nature Communications *5*, 3035.
DOI: 10.1038/ncomms4035

Weber, K.A., Achenbach, L.A., Coates, J.D. (2006). Microorganisms pumping iron: anaerobic microbial iron oxidation and reduction. Nature Reviews Microbiology *4*, 752-764.
DOI: 10.1038/nrmicro1490

Weber F.A., Hofacker A.F., Kretzschmar R. (2010). Temperature dependence and coupling of iron and arsenic reduction and release during flooding of a contaminated soil. Environmental Science & Technology 44, 116-122.
DOI: 10.1021/es902100h

Wickham, H. (2009). Getting started with qplot. In ggplot2, (Springer New York), pp. 9–26.

World Health Organization. (2011). *Guidelines for drinking-water quality*. World Health Organization, Geneva, p.135.

Yang, W.H., Weber, K.A., and Silver, W.L. (2012) Nitrogen loss from soil through anaerobic ammonium oxidation coupled to iron reduction. Nature Geoscience Letters *5*, 538-541.
DOI: 10.1038/ngeo1530